# A WESTERBORK SURVEY OF CLUSTERS OF GALAXIES I. 21 CM OBSERVATIONS OF A1656, A2147, A2151, A2197 AND A2199: RADIO DATA AND IDENTIFICATIONS

#### W.J. JAFFE

Sterrewacht, Huygens Laboratorium, Leiden, The Netherlands and

G.C. PEROLA

Istituto di Scienze Fisiche and Laboratorio di Fisica Cosmica e Technologie Relative, Milan, Italy

Received February 5, 1975

As a part of a programme of radio observations of rich clusters of galaxies, we have observed 5 nearby Abell clusters at 21 cm wavelength using the Westerbork Synthesis Radio Telescope. The angular resolution was  $23'' \times 23''$  cos  $\delta$  and the ultimate detection limit was 2.4 mJy. Here we describe the observing and reduction techniques, and present a list of all detected radio sources, along with contour maps of the more extended sources. An identification search was carried out on the Palomar Sky Survey prints and on deep 48" IIIaJ Schmidt plates. For each identification we present optical data and include a finding chart. A total of 27 probable cluster members was detected.

Key words: radio source survey - clusters of galaxies - identifications

#### 1. INTRODUCTION

We have undertaken a programme of high resolution-high-sensitivity observations of nearby rich clusters of galaxies using the Westerbork Synthesis Radio Telescope (WSRT). The main purpose of this project is to determine the luminosity function (down to powers at 21 cm of the order  $10^{20} - 10^{21}$  Wm<sup>-2</sup>Hz<sup>-1</sup>st<sup>-1</sup>) and the morphology of radio sources in clusters. This information will then be compared with that available on field galaxies to investigate the existence of a connection between the radio properties of galaxies and their membership to a cluster.

The first such general study of cluster radio sources was made by Willson (1970) using the Cambridge One-Mile Telescope to observe the cluster Abell 1656 in Coma Berenices. We hope to extend Willson's survey by using the high sensitivity and stability of the WSRT to yield more detected radio sources and to improve the positional accuracy of those found. We have also observed four new clusters, A2147, A2151 (together making up the Hercules cluster), A2197 and A2199. Preliminary results of some of these observations at 21 cm wavelength were given in Jaffe and Perola (1974). Here we give more details on the observation and reduction technique, present a list of all radio sources detected, and present the results of a search for identifications of the radio sources with optical sources visible either on the Palomar Sky Survey or, in the case of the clusters A1656, A2147, or A2151, objects visible on deep 48" Schmidt plates taken by F. Bertola. Where available, we have included data on the identified objects from other sources.

In later papers we will discuss the statistical results derivable from these data, and present reobservations of several of these clusters with the WSRT at 50 cm wavelength.

## 2. OBSERVATIONS

The operations of the WSRT is described in detail elsewhere (Högbom and Brouw 1974). Very briefly, the instrument consists of twelve 25<sup>m</sup> parabolic dishes on an east-west line. Ten of these dishes are fixed

at 144 m intervals on the ground, two movable dishes 72 m apart are mounted on a rail beginning 27 m east of the last fixed telescope.

The signals from each fixed telescope are correlated with those from each movable telescope providing simultaneous interferometric measurements on 20 baselines at 72 m intervals. After following a region of the sky for 12 hours we have measurements along 20 ellipses in the UV plane spaced 72 m apart along their major (east-west) axes and 72 m sin  $\delta$  along their minor (N-S) axes, where  $\delta$  is the declination of the field centre. By shifting the movable telescopes and reobserving the field we obtain another set of 20 ellipses which can be used to fill the gaps between the first days' measurements. In this way we obtain after two half-days' measurements observations spaced 36 m apart along the E-W axis, and after four half-days observations spaced 18 m apart. These spacings produce elliptical "grating ring" artifacts around every source in the computed maps. At 21 cm for  $2 \times 12$  hr observations these rings are 40' across in R.A. by 40' csc  $\delta$  in declination. For a  $4 \times 12$  hr observation the rings are twice as large.

In table 1 we list the specifications of all the measurements made.

#### 3. CALIBRATION

The exact position of the 12 telescopes on the ground and the gain and instrumental phase of the receivers were derived from regular observations of 3C 48 and 3C 295 for which the following parameters were assumed:

	R.A.	Dec.	Flux density
3C 48	1 <sup>h</sup> 34 <sup>m</sup> 49 <sup>s</sup> .82	+ 32°54′20″2	15.6 Jy
3C 295	14 <sup>h</sup> 09 <sup>m</sup> 33 <sup>s</sup> .44	$+52^{\circ}26'13''.6$	-

The quality of the calibrations is such that, assuming the calibration source parameters to be exact, the individual receiver phases are determined to about 4° accuracy, the individual receiver gains to about 5% and the baseline parameters to about 4 mm. In practice these uncertainties mean that artifacts are produced in the calculated maps whose apparent flux densities are as high as 0.5% of the peak strength of the strongest source in the field. In some fields it is these artifacts which limit the completeness of the survey rather than the system noise.

Furthermore the absolute positions of the calibrator sources were uncertain by about 0".5 and the flux of 3C 48 by about 5%. These uncertainties do not affect the relative positions and fluxes of sources in a given field and do not create artifacts, but do imply that the absolute positions and fluxes of the sources may be in error by similar amounts.

#### 4. MAPS AND ANTENNA PATTERNS

The calibrated measurements were Fourier transformed, as described by Högbom and Brouw (1974) to provide maps of sky brightness. For each observed field an antenna pattern, the response of the telescope to a point source of unit flux density, was also constructed. In general the antenna pattern has a central peak whose FWHP is about 23" in R.A. and 23" csc  $\delta$  in Dec. The first two sidelobes have heights of -5% and +3% of the central peak, and are located 1.5 and 2.5 beamwidths away from it. The antenna pattern also contains the grating rings described earlier. The details of the antenna patterns depend on the baselines and hour angles measured for each field, on the relative weights assigned to the various measured points and, to a smaller extent, on the numerical technique used in realizing the Fourier transform.

#### 5. NOISE AND SYSTEM IMPERFECTIONS

The effective noise in the maps were determined by making a gaussian fit to the counts of very weak deflections in the transformed map of the observations of A2197. This revealed an rms noise in the map of  $\sigma_{2197} = (0.55 \pm .02)$  mJy. Other maps combining 4 half-days' observations had similar noise levels. A2147, observed for only  $2 \times 12$  hr had a noise level  $\sqrt{2}$  times higher. A1656 (Coma) was observed for  $5 \times 12$  hr but the observations could not be eqally weighted and still provide a uniform coverage of the UV plane, hence the improvement in system noise over the  $4 \times 12$  hr measurements was marginal. Furthermore, the intersection of the grating rings from the large number of weak sources in the Coma field served as a source of "confusion noise" which in fact increased the rms noise level to  $\sigma_{1656} = 0.6$  mJy.

In two of the fields, A2151 and A2199, artifacts due to inaccurate calibrations appeared around the strong sources at the centers of these fields. The maximum levels of these artifacts were equivalent to sources of about 3.4 mJy and 5 mJy for A2151 and A2199 respectively. For this reason the searches of these fields were terminated at map fluxes of 5 mJy so that no spurious sources would be included. Furthermore the searches cannot be considered complete to 5 mJy because in some of the strongly disturbed areas of the map sources of this map flux could not be detected.

#### 6. SOURCE PARAMETER EXTRACTION

The transformed maps were searched for points whose computed intensities exceed a certain minimum value, determined as described below. At each such point, making use of the computed antenna pattern, the computer finds the flux density and position of the point source which best reproduces the transformed intensities at that point and a group of surrounding points. It also estimates the errors in the flux and positions. Areas of the maps disturbed by instrumental artifacts were excluded from this analysis.

Where the grating rings of a strong source confused the search for weak sources, the strong source and its grating ring were subtracted from the map using the theoretical antenna pattern. Where the disturbing source was extended it was decomposed into a number of point sources and these were subtracted. On the resulting "cleaned" map the search was repeated down to a lower level.

Fields free of disturbing instrumental imperfections were searched and cleaned as described above to detect all sources above 4  $\sigma$  in a 1°1 (R.A.) by 1°4 (Dec.) rectangle about the field center. As mentioned above the fields A2151 and A2199 were searched only for sources above 5mJy. The extent in R.A. was smaller than that in Dec. because "aliasing" effects due to the numerical Fourier transform technique used, increased the noise near the edge of the transformed field, and provide the possibility that a source just outside the transformed field is erroniously located at another point just inside the field. Because of the lower resolution of the Synthesis instrument in the declination direction, a much larger extent in this direction could be included in the numerical transforms and the aliasing effects were small up to 0°.7 from the field center, where the telescope attenuation cuts off the usable field.

In addition to the searches, contour maps of each field were made in order to identify extended sources and to estimate the degree to which the maps were affected by grating rings and instrumental effects. Where the contour maps indicated that a source might be extended the following procedure was used to measure the extension and the total flux density of the source. A rectangular region surrounding the source and containing at least all points within the first closed 0— contour around the source was selected and Fourier transformed back to the UV plain to yield a smoothed estimate of the visibility amplitude of the source as a function of interferometer baseline and hour angle (or equivalently, as a function of U and V). For a point source this visibility amplitude is constant for all U and V; for a resolved source the amplitude drops with increasing baseline and drops most quickly at an hour angle corresponding to the position angle of the maximum extent of the source. To search for this effect we fitted a second order, two-dimensional polynomial

in U and V to the smoothed visibility amplitude A(U,V) to find the best least-square values of the parameters A(U=0,V=0),  $\partial^2 A/\partial U^2$  (0,0),  $\partial^2 A/\partial V^2$  (0,0), and  $\partial^2 A/\partial U\partial V$  (0,0).

Where either  $\partial^2 A/\partial U^2$  or  $\partial^2 A/\partial V^2$  exceeded 2.5 times the rms uncertainty in their estimation the source was considered extended. A (0,0) was then used as the best estimate of the total source flux and the second derivatives of A were used to determine the degree of extension. Where neither derivative exceeded 2.5 times the noise, the source was considered unresolved and the flux determined by the normal search program was used.

The second derivatives of the visibility amplitude contain all the significant information which can be determined for slightly extended sources. The second derivatives are, however, proportional to the total flux of the source and to the square of the source dimensions. As a measure of extension which is independent of source flux we define the source parameters  $D_{\alpha} = ((\partial^2 A/\partial U^2)/A)^{1/2}/\pi$ , and  $D_{\delta} = ((\partial^2 A/\partial V^2)/A)^{1/2}/\pi$ . One can show that for a source consisting of two equal point sources,  $D_{\alpha}$  and  $D_{\delta}$  would be equal to the projected separation of the points in the R.A. and Dec. directions respectively.

Where only one of  $\partial^2 A/\partial U^2$  or  $\partial^2 A/\partial V^2$  could be determined from the measurements, then the equivalent parameter  $D_{\alpha}$  or  $D_{\delta}$  is given in column 10 of table 2. Where all of the second derivatives could be determined the position angle p of the major axis of the extension was found. In this case column 10 contains the D parameter measured along this axis, the D parameter measured perpendicular to the major axis (given as 0'' if no extension could be detected in this direction), and the positional angle p.

For very extended sources (with dimensions larger than one beamwidth) the second derivatives are inadequate to describe all information about the extension. For uniformity and for ease of comparison with measurements at lower resolution we have also determined the *D* parameters for these sources, but in addition we include in table 2 a short description of the source structure and in figure 5 give a contour map of the source superimposed on a 48" Schmidt photograph of the same region of sky.

The noise limits the detection of extension to sources for which  $D_{\alpha} > 40'' (\sigma/S_m)^{1/2}$  or  $D_{\delta} > 40'' (\sigma/S_m)^{1/2}$  csc  $\delta$ , where  $S_m$  is the source map flux and  $\sigma$  is the rms uncertainty in the measurement of the flux of a point source (see section 5).

The above method of determing total map flux and extension of sources is quite simple and consistent for slightly extended sources (with dimensions less than one beamwidth) and is not very sensitive to the exact region which is Fourier transformed so long as this is substantially greater than the beamwidth (in general we used a  $4 \times 4$  beamwidth area). On the other hand, this method, like all others for determining the parameters of extended sources, is highly sensitive to instrumental effects and defects present in the area around the source, such as grating rings of other sources, offset zero levels and so forth. These problems must be dealt with using "scientific judgement".

For sources which are, or might be, highly extended, the choice of the appropriate area to transform is difficult. These sources might, for instance, have large low surface brightness extensions which are not recognizable above the noise and whose omission leads to an underestimate of the total flux. This means that the fluxes of weak sources larger than the minimum transformed area (4×4 beamwidths) will be systematically low. We believe, however, that the number of such weak very extended sources is small since the percentage of strong very extended sources, where the extension is recognizable, is small (about 5% of sources with map fluxes above 10 mJy) so that the effect of such weak sources on the statistical conclusions which can be drawn from this data should be small.

After the map fluxes  $S_m$  were determined for all sources these were converted to sky fluxes  $S_s$  by correction for the attenuation of the telescope response pattern. This was done with the aid of a programme developed by C. Oosterbaan of Leiden University which takes into account the single dish antenna responses of each telescope and the variation of distance of each source from each telescope steering center as a function of time due to small errors in the telescope steering program. The sky fluxes  $S_s$  along with the map fluxes  $S_m$  are given in columns 7 and 9 of table 2.

The use of this programme eliminates, at least on the average, the discrepancy between Westerbork fluxes and 5C4 fluxes in the Coma field mentioned in Jaffe and Perola (1974). Figure 1 shows the relation between

the Westerbork 1415 MHz fluxes and the revised Cambridge 1407 MHz fluxes (Gillespie 1974) for sources in common in the present survey and the 5C4. The agreement is on the whole satisfactory.

## 7. FLUX AND POSITION ERRORS

The flux and position determinations are subject to errors due to noise and to instrumental calibration errors. The rms errors due to the noise in the map fluxes of point sources are equal to the noise values  $\sigma$  found in section 5. For extended sources the uncertainties in flux are larger essentially because the signal from the long baseline interferometers cannot be used with full weight in calculating the total flux. For slightly extended sources, the uncertainty in the fluxes derived as described in section 6 is about 1.5 times larger then the uncertainty for a point source. For very extended sources the uncertainty is approximately  $(1+D_{\alpha}D_{\delta}\sin\delta/(23'')^2)^{1/2}$  times that for a point source. In addition to these uncertainties due to noise, the map fluxes may be in error up to about 5% due to imperfections in the calibration procedure.

The sky flux of each source is derived from its map flux and from the correction for the primary beam attenuation pattern. The errors in the sky fluxes, listed in column 8 of table 2 are thus equal to the errors in the map fluxes multiplied by the beam correction factor, combined with the errors due to the uncertainties in the attenuation factor itself. Estimates of these last errors have been derived from a few test fields in other observation programmes where observations of the same source at various distances from the field centers were available. These tests indicate that the uncertainty in the attenuation pattern is of the order of 3% for attenuation factors less than 2, about 6% for factors between 2 and 10, and of the order of 20% for factors between 10 and the maximum found in the survey, which is about 20.

The search programme estimates the position errors due to noise on the basis of a quality of fit test. It calculates those displacements in  $\alpha$  and  $\delta$  which produce residuals in fitting of the antenna pattern to the measured intensities which are of the same magnitude as the residuals due to noise alone. Since the estimates of the position errors so calculated are also subject to noise fluctuations, the errors quoted in table 3 are an average of the errors estimates for all sources in the same field of approximately the same map flux density. The relations between map flux and the error in  $\alpha$  for the various fields are shown in figure 2. The errors in  $\delta$  are approximately equal to those in  $\alpha$  multiplied by the ratio of the beamwidths in  $\delta$  and in  $\alpha$ , which is  $\csc \delta$ .

For very bright sources the calculated errors, due only to noise, become very small. For these bright sources the principal source of error comes from the calibration errors in the Westerbork clock, frequency, and baseline parameters. These and the uncertainties in the absolute celestial positions of the calibrating sources set a lower limit of about 0.5 on the error in  $\alpha$ , and 0.5 csc  $\delta$  on the error in  $\delta$ .

## 8. COMPLETENESS

Except in the "disturbed areas" the survey should include all sources whose peak apparent map fluxes, i.e. true peak map flux plus superimposed noise, exceeds four times the rms noise in the map in the case of A1656, A2147, and A2197, or exceeds 5 mJy for A2151 and A2199, and which are located within a 1°.4 (Dec.) by 1°.1 (R.A.) rectangle about the field center. Because of the attenuation of the single dish primary beams, the map flux of a source with a given sky flux decreases as the source is moved away from the field center. For this reason stronger sources are detectable at larger radii than weaker sources. This effect is plotted in figure 3, where the maximum distance from the field center within which a source would have a true map flux above the survey cutoff limit is given as a function of the source sky flux. In reality the presence of noise superimposed on the sources means that some sources with true map fluxes slightly greater than the detection limits have been omitted while other sources with true fluxes just under these limits have been included.

## 9. OPTICAL IDENTIFICATIONS

The optical material directly used for the identifications consisted of 48" Palomar III a-J plates of the Coma and Hercules Clusters (kindly lent to us by F. Bertola) and of the red N.G.S. Palomar Sky Survey print of A2197–2199.

The identification programme was carried out with the X-Y measuring machine at Bologna, RAUB. The plate constants were first obtained by measuring the coordinates of a suitable number of reference stars, from the AGK 2 catalogue. Then the celestial coordinates of the objects close to the radio position were measured. The optical positions obtained were accurate within  $\sigma_0 = 0.8-1''$ , in both  $\alpha$  and  $\delta$ . While this is a fair estimate of the accuracy for points and spherically symmetric images, the precision in the position of the centroid of diffuse non-spherical images is inferior.

In addition we produced high contrast blow-ups ( $\times$  30) of the optical fields around each radio source, that were used as a control for very weak objects which might have been missed under the microscope, and to determine the nature of the optical objects.

We have subdivided the possible identifications into three classes. Class I contains the identifications of unresolved radio sources which satisfy the criterion

$$\frac{\Delta \alpha^2}{\sigma_{\alpha}^2 + \sigma_{o}^2} + \frac{\Delta \delta^2}{\sigma_{\delta}^2 + \sigma_{o}^2} \le 9$$

where  $\Delta \alpha = \alpha_o - \alpha_R$ ,  $\Delta \delta = \delta_o - \delta_R$  are the difference between the optical and radio coordinates. For  $\sigma_\alpha$  and  $\sigma_\delta$ , the errors in radio position, the values given in table 2 were used, and for  $\sigma_o$  an error of 1" in both coordinates, irrespective of the type of the optical image, was adopted. Class II includes:

- a) Unresolved sources not meeting the above criterion, but well inside the optical image of a galaxy.
- b) Extended radio sources, when the optical object lies close to the radio centroid.

Class III includes:

- a) Unresolved radio sources between 3 and 4 $\sigma$  away from an object, or in the outer envelope of a galaxy.
- b) Extended radio sources with an outstanding object nearby, but far from the radio centroid. This class includes also the strong radio source 1600+16 W2, less than 6'' away from a faint blue object, that due to the very small error in radio position lies outside  $4\sigma$ .

Class III was introduced in an attempt to recover, at the risk of including an uncertain number of spurious identifications, some of those objects that on the basis of pure positional coincidence, would have been missed either because a second radio component was below the detection limit, or because of a displacement of the radio emitting region with respect to the optical object.

The identified radio sources are listed in table 3. For detailed information on the sources 1256 + 28W9 (N4869), 1257 + 28W1 (N4874), 1602 + 17W4 (N6047) and 1626 + 29W3 (N6166) see Jaffe and Perola (1974).

Column 1: name of source

Column 2: combined (radio + optical) errors in position, only for unresolved sources

Columns 3 and 4: celestial coordinates of optical object (1950)

Columns 5 and 6: difference between R.A. and Dec. of optical object and radio source. (arcsec)

Column 7: identification class

Column 8: comments on optical object. The sources of information are referred to by means of superscripts (see note to table). The morphological type of the galaxies and the magnitudes, when not available from the literature, were tentatively inferred from the material used for the identifications and the P.S.S. prints. For objects visible only on the IIIa-J plates, the estimated magnitude is given as  $m_g(g = \text{green})$ . Uncertainties:  $\pm 1^m$  for galaxies and  $\pm 0^m$ .5 for stellar images. The symbols (F) and (M) mean respectively that a finding chart or a radio map superimposed on the optical field is reproduced in figures 4 or 5. The radial velocities v

are relative to the origins used by the original observers. These are indicated below. References in the table are:

- a) Zwicky and Herzog (1963)
- b) Tifft and Tarenghi (1974) (v relative to galactic center).
- c) Willson (1970)
- d) Bautz (1972) (v relative to Sun)
- e) Burbidge and Burbidge (1959) (v relative to galactic center)
- f) Corwin (1971)
- g) Chincarini and Rood (1972) (v relative to center of local group)
- h) RB = Rood and Baum (1967)
- i) RS = Rood and Sastry (1972)
- j) Tifft (1974) (v relative to galactic center)

Although the radio error boxes at 21 cm are small, the contamination by chance coincidences even in class I is not negligible. On the material used for the identifications the number of objects down the plate limit was estimated by counting the number of objects in randomly distributed areas of 10<sup>5</sup> arcsec<sup>2</sup> (see table 4). In each field the unresolved radio sources were subdivided into groups according to their position errors, and for each group the number of expected chance identifications was found. The results are given in table 4. The first column gives the position error for the group, the second column the total number of radio sources in each group including unresolved components of sources classified as double, the third column the number of expected chance class I identifications, and the fourth column the number of class I identifications actually found. Separate comments on each observed field are:

Coma: out of a total of 13 identifications, 3 to 4 (30%) could be due to chance. We expect 90% of these chance identifications would be with faint objects (m > 19). However, of the 5 such objects found, 4 are group 4 objects, with very small position errors, where only 0.4 chance identifications are expected, and 1 (1257 + 27W2) is a group 1 object. Taking this into account we expect only one or two of the identifications to be fortuitous.

A2197–2199: out of a total of 9 identifications about 2 should be spurious. The most likely candidates are again the faintest objects.

A2147-2151: out of a total of 18 identifications 8 are expected to be spurious (44%). Since in each group the number of identifications with objects of m > 19.5 is close to the NEI, most of these faint identifications are probably fortuitous.

However, for the galaxies with m < 19, in each field, the probability of a chance coincidence is negligibly small, and practically zero for galaxies with  $m \le 17$ , 28 cases.

In the next paper in this series we will discuss the statistical information contained in the source and identification lists presented here. In particular we shall attempt to derive the radio luminosity function for the cluster galaxies and the  $\log N - \log S$  relation for the sources not directly associated with cluster galaxies. We shall also investigate the angular size properties of both cluster and non-cluster radio sources.

### **ACKNOWLEDGEMENTS**

The authors wish to thank Prof. H. van der Laan for stimulating them in beginning this project. They also wish to thank Prof. F. Bertola for providing them with two of his plates, the Bologna Group, RAUB, and especially Dr. L. Formiggini for their help in the identification programme, and N. Primavera and J.F. Planken for their photographic work. G.C.P. wishes further to thank the Sterrewacht of Leiden for its hospitality, and to acknowledge financial support from the Italian Consiglio Nazionale delle Ricerche, and a two month grant from the Netherlands Organization for Pure Research (Z.W.O.) The Westerbork Radio Observatory and Reduction Group are administered by the Netherlands Foundation for Radio Astronomy (S.R.Z.M.) with the financial support of the Z.W.O. The authors wish also to thank Dr. R. Allen for his role in initiating this project.

# **REFERENCES**

Bautz, L.P.: 1972, Astron. J. 77, 331.

Burbidge, G.R. and Burbidge, E.M.: 1959, Astrophys. J. 130, 629.

Chincarini, G. and Rood, H.J.: 1972, *Astron. J.* 77, 448. Corwin, H.G. Jr.: 1971, *Publ. Astron. Soc. Pacific* 83, 320.

Gillespie, A.R.: 1974, private communication.

Högbom, J.A. and Brouw, W.N.: 1974, Astron. Astrophys. 33, 289. Jaffe, W.J. and Perola, G.C.: 1974, Astron. Astrophys. 31, 223.

Rood, H.J. and Baum, W.A.: 1967, Astron. J. 72, 398. Rood, H.J. and Sastry, G.N.: 1972, Astron. J. 77, 451.

Tifft, W.T.: 1974, Astrophys. J. 188, 221.

Tifft, W.T. and Tarenghi, M.: 1975, submitted to Astrophys. J. Willson, M.A.G.: 1970, Monthly Notices Roy. Astron. Soc. 151, 1.

Zwicky, F. and Herzog, E.: 1963, Catalogue of Galaxies and Clusters of Galaxies, Vol. 2 and 3, Calif. Inst. of Technology, Pasadena.

W.J. Jaffe

Sterrewacht

Huygens Laboratorium Wassenaarseweg 78

Leiden 2405, The Netherlands

G.C. Perola

Istituto di Scienze Fisiche Via Celoria 16 Milano 20133, Italy

Table 1 WSRT observations used in this survey

Field	Observation Date	Baseline Coverage	(m)	Hour Cover	Angle age	Field Center (1950) R.A. Dec.
A1656	70207	72 ( 72)	1296	-83°	+90°	12 <sup>h</sup> 56 <sup>m</sup> 36.01 28 <sup>o</sup> 11'42.2
A1656	70228	180 ( 72)	1548	-90	+90	
A1656	70258	198 (72) 1	566	-90	+90	
A1656	70264	90 ( 72)	1458	-90	+90	
A1656	72034	36 ( 72)	1404	-90	+90	
A1656	72068	102 ( 72)	1470	-90	-70	
A2147	72035	36 ( 72)	1404	-90	+90	16 01 13.51 16 17 48.2
A2147	72058	72 ( 72)	1440	-90	+90	
A2151	70208	72 ( 72)	1440	-90	+90	16 02 52.03 17 53 00.2
A2151	70227	180 (72)	1548	-90	+90	
A2151	70256	198 ( 72)	1566	-90	+90	
A2151	70262	90 ( 72)	1458	-90	+90	
A2197	70284	180 ( 72)	1548	-90	+90	16 28 06.06 40 55 04.4
A2197	70313	234 ( 72)	1602	-90	+90	
A2197	70342	216 ( 72)	1584	-90	+90	
A2197	71006	198 (144)	1494	-90	-72	
A2197	71007	198 (144)	1494	-72	-64	
A2197	71288	198 ( 72)	1566	-64	+90	
A2199	70215	72 ( 72)	1440	-77	+90	16 26 55.32 39 39 20.0
A2199	70229	180 ( 72)	1548	-54	+90	
A2199	70249	180 ( 72)	1458	-90	+90	
A2199	70257	198 ( 72)	1566	-90	+90	
A2199	70263	90 ( 72)	1458	-90	+90	

Note: "Observation Date" 70207 means year 1970, sidereal day 207;

"Baseline Coverage" 180 ( 72) 1548 means that all baselines
between 180 m and 1548 m at 72 m intervals were measured.

Table 2 21 cm cluster radio source list

Field (1)	l Name (2)	α. (3)	σ <sub>α</sub>	8	σδ.	Ssky	σ (8)	s map (9)	Comments
		(3)	(4)	(5)	(6) ———	(7)	(8) ———	(9)	(10)
1	1254+27W1	12 54 59.06	.11	27 46 08.1	3.1	58.2	7.	5.0	5C4.51
1	1254+28WIa b	12 54 10.82 12 54 13.93	.19 .14	28 32 46.3 28 32 57.8	5.4 4.0	71.3 87.7	15. 14.	2.9 3.9	Asym. double sep. 40", p.a. $70^{\circ}$ (M) D <sub>\alpha</sub> = 24", 5C4.42
1	1254+28W2	12 54 50.25	.16	28 02 44.7	4.5	12.5	2.2	3.4	
1	1255+27W1	12 55 29.75	.20	27 53 17.9	5.6	9.0	2.0	2.7	
1	1255+27W2a Ъ	12 55 46.88 12 55 49.55		27 50 57.4 27 51 39.6		28.8 12.9	3.0 1.0	8.6 3.8	Asym. double sep. 40", p.a. 30° (M) possible 3 <sup>d</sup> component, D=(26",14",20°),5C4.62
1	1255+28W1	12 55 20.26	.05	28 13 52.2	1.4	19.1	0.9	10.9	5C4.53
1	1255+28W2	12 55 27.51		28 22 22.0	1.2	64.3	1.2	33.5	$D_{\alpha} = 10^{11}, 5C4.54$
1	1255+28W3	12 55 32.01	.25	28 19 49.0	7.1	3.9	1.0	2.4	
1	1255+28 <b>W</b> 4a b	12 55 35.24 12 55 37.06	.12 .05	28 37 17.4 28 36 13.8	3.4 1.4	20.5 51.1	3. 3.	3.9 11.0	Asym. double sep $68"$ , p.a. $160^{\circ}$ (M) $D=(21",0",160^{\circ}),5C4.57$
1	1255+28W5	12 55 39.27	.22	28 06 27.6	6.2	3.6	0.8	2.5	
1	1255+28W6	12 55 40.63	.07	28 30 49.1	2.0	20.8	1.6	7.7	5C4.58
1	1255+28W7	12 55 47.14	.07	28 44 00.0	2.0	80.0	9.	7.2	5C4.61
1	1256+27W1	12 56 14.17	. 19	27 55 49.4	5.4	5.3	1.0	2.9	
1	1256+27W2	12 56 34.40	. 19	27 58 27.2	5.4	4.3	0.8	2.8	
1	1256+27W3	12 56 37.98	.17	27 47 52.4	4.8	11.6	1.7	3.2	5C4.78
)	1256+27W4	12 56 40.23	.23	27 54 50.2	6.5	4.7	1.9	2.4	
1	1256+28W1	12 56 17.25		28 10 17.6		29.0	1.5	27.0	$p_{\alpha} = 10'', 5C4.70$
1	1256+28W2	12 56 28.22	.21	28 10 53.1	6.0	2.7	0.6	2.6	5C4.72?
1	1256+28W3	12 56 29.34	.04	28 34 02.8	1.1	70.3	1.6	27.0	5C4.73
1	1256+28W4a b	12 56 32.73 12 56 36.00		28 03 03.1 28 02 43.4		71.7	3.5	58.5	Double (M) D=(26 <sup>o</sup> ,0 <sup>o</sup> ,105 <sup>o</sup> ) flux ratio 1.2:1 5C4.74ab
1	1256+28W5	12 56 33.35	.10	28 35 40.0	2.8	16.0	1.8	5.3	5C4.75
1	1256+28W6	12 56 36.36	.07	28 27 49.9	2.0	13.1	1.0	8.1	5C4.77
1	1256+28W7	12 56 37.24		28 23 09.4		11.2	1.	8.7	D <sub>a</sub> =10"
1	1256+28W8	12 56 55.23	.16	28 21 15.4	4.5	4.1	0.7	3.3	
1	1256+28W9	12 56 56.5		28 10 40		450	20.	425.	5C4.81 see Jaffe and Perola (1974)
1	1257+27W1	12 57 18.29	.19	27 57 30.9	5.4	5.2	1.0	2.9	
1	1257+27W2	12 57 42.09	.06	27 45 44.6	1.7	68.7	4.0	8.8	5C4.92
1	1257+27W3	12 57 49.91	.07	27 55 46.4	2.0	23.0	1.6	8.0	5C4.95
1	1257+28W1	12 57 10.8		28 13 40		215.	10.	184.	5C4.85, D= $(13'',6'',40^{\circ})$ see Jaffe and Perola (1974)
1	1257+28W2	12 57 40.22	.23	28 04 18.9	6.5	4.4	0.9	2.4	
1	1258+27W1	12 58 56.25	.14	27 53 29.1	4.0	84.6	12.	4.1	5C4.128
1	1258+28W1	12 58 01.82	.10	28 25 30.7		17.2	1.6	5.7	5C4.102
1	1258+28W2	12 58 03.93	.10	28 46 19.4	2.7	160.	18.	5.5	edge of field, 5C4.105
1	1258+28W3	12 58 13.39	.08	28 19 31.8	2.1	20.8	1.6	7.1	5C4.108
1	1258+28W4	12 58 15.57	.10	28 16 23.7	2.8	15.0	1.6	5.2	5C4.111

Table 2 (continued)

Field (1)	Name (2)	α (3)	σ <sub>α</sub> (4)	δ σ (5) (6	δ S	sky (7) (	s 8)	тар (9)	Comments (10)
	1258+28W5	12 58 2	6.18 .05	28 24 10.1	1.4	50.7	2.8	10.7	5C4.114
	1258+28W6	12 58 3		28 03 36.8		17.3	3.0	3.5	504.117
1	1258+28W7		7.14 .12	28 23 32.8		50.6	6.0	4.6	5C4.129
•	1230120#7	12 30 3	7.14 .12	20 23 32.0	3.4	30.0	0.0	4.0	3341.25
2	1559+15W1	15 59 0	6.82 .10	15 45 13.8	4.9	560.	70.	6.4	edge of field, 4C+15.52, OR+198.5
2	1559+15W2	15 59 5	5.89 .18	15 58 25.6	8.8	14.1	3.2	3.5	
2	1559+16W1	15 59 5	6.88 .18	16 09 22.2	8.8	7.5	1.6	3.5	
2	1559+16W2a b	15 59 5 16 00 Q		16 06 14.2 16 07 16.2		33.0	4.0	15.0	Double,flux ratio 1:1.3 (M) D = (35,15,25°)
2	1600+15W1	16 00 1	1.56 .15	15 52 21.4	7.6	23.1	4.1	4.1	
2	1600+15W2	16 00 1	9	15 52 12		887.	40.	175.	very extended (M), D = (51,45", 124°) 4C+15.53, OS+101
2	1600+16W1	16 00 0	1.47 .03	16 15 27.5	1.7	30.7	1.4	16.3	
2	1600+16W2	16 00 0	1.66 .03	16 11 36.9	1.7	33.1	1.4	18.2	
2	1600+16W3	16 00 2	9	16 11 24		20.0	2.0	15.5	Extended, triple?, (M), $D_{\alpha} = 46$ "
2	1600+16W4	16 00 2	6.13 .16	16 29 30.1	7.8	6.8	1.2	4.0	
2	1600+16W5	16 00 2	7.87 .05	16 15 55.8	2.5	17.2	1.0	14.0	Extended,D <sub>a</sub> =10"
2	1600+16W6	16 00 3	8.42 .17	16 36 56.1	8.4	9.5	1.8	3.8	
2	1600+16W7	16 00 4	1.19 .19	16 29 03.7	9.3	4.9	1.0	3.4	
2	1600+16W8	16 00 4	1.78 .17	16 20 35.1	8.3	4.2	1.0	3.7	
2	1600+16W9	16 00 5		16 06 08.3		34.8	1.0	25.5	
2	1600+16W10	16 00 5		16 32 24.7	4.2	11.6	1.2	7.2	(x) (//H 20H 20 <sup>Q</sup> )
2	1600+16W11	16 00 5		16 12 00		41.7	2.	39.0	Extended (M), D = (44", 33",80°)
2	1601+15Wla b	16 01 2 16 01 2		15 55 52 15 55 52		110.	6.	43.5	Double (M), flux ratio 1:1.2, D <sub>α</sub> =43"
2	1601+15W2	16 01 4	1.07 .04	15 55 44.1	2.0	41.2	2.2	14.7	
2	1601+15W3	16 01 4	5.30 .10	15 55 09.6	4.9	19.0	2.5	6.2	
2	1601+16W1	16 01 1	1.91 .03	16 43 33.7	1.7	73.1	3.0	17.0	
2	1601+16W2	16 01 2	0.90 .11	16 16 00.1	5.4	5.6	0.8	5.5	
2	1601+16W3	16 01 2	0.90 .03	16 02 16.1	1.7	89.3	3.	57.8	
2	1601+16W4	16 01 2	6.22 .11	16 12 36.8	5.4	5.9	0.8	5.5	
2	1601+16W5	16 01 3	5.89 .03	16 28 12.1	1.7	78.5	1.5	58.0	
2	1601+16W6	16 01 5	0.99 .07	16 05 04.5	3.3	14.4	1.2	9.1	
_	1601+17WI		6.26 .07	17 20 12.1		410.	30.	9.8	
3	1601+18W1	16 01 3	33.51 .08	18 00 45.0	3.9	17.1	1.4	7.6	
	1602+15W1		3.52 .03	15 54 30.0	1.7	111.1	5.	24.0	
	1602+16W1	16 02 0	00.23 .05	16 18 37.3	2.2	18.2	1.	14.0	
	1602+16W2	16 02 0	9.89 .12	16 08 52.7	5.9	10.4	1.4	6.0	
2	1602+16W3	16 02 1	1.94 .13	16 13 55.5		7.4	1.1	4.8	
	1602+16W4	16 02 3	39.40 .12	16 18 50.1		13.2	1.8	5.3	_
3	1602+17W1	16 02 1	1.41 .03	17 52 39.4	1.7	133.	2.	107.	Extended, D = $(17'', 0'', 4^{\circ})$

Table 2 (continued)

Field (1)	Name (2)	(3)	σ <sub>α</sub> (4)	δ (5)	<sup>σ</sup> δ (6)	S sky (7)	σ (§)	s (9)	Comments (10)
3 1	602+17W2	16 02 20.51	.09	17 51 13.0	4.7	7.8	1.0	6.7	
	602+17W3	16 02 21.34	.05	17 41 28.4		19.7	0.8	12.4	
_	602+17₩4	16 02 53.98	.05	17 51 53.5		766.	30.	766.	Extended, D=(21", 7",5°),4C17.66 c.f. Jaffe and Perola (1974)
3 1	602+18W1	16 02 10.86	.06	18 11 24.8	2.9	26.9	2.6	12.2	Extended, D <sub>a</sub> = 8"
	602+18W2	16 02 21.55	.03	18 06 34.4		26.8	1.0	17.5	α
	603+17W1	16 03 03.81	.03	17 39 50.7		37.9	1.0	23.5	
_	603+17W2	16 03 22.00	.18	17 56 25.7		4.3	0.8	3.5	Flux below survey completeness limit,
	603+17W3	16 03 29.91	.09	17 50 42.9	4.4	8.8	0.8	6.9	included because of interesting identification
	603+17W4	16 03 41.35	.08	17 48 07.0		12.1	0.8	8.1	
3 1	603+17W5	16 03 46.03	.03	17 55 49.0		121.	2.	88.5	Extended, D <sub>8</sub> = 16"
3 1	603+18W1	16 03 11.60	.10	18 03 47.6	4.9	7.8	0.8	6.1	
3 1	603+18W2a b	16 03 24.6 16 03 27.2		18 20 08.2 18 20 24.3		63.2	6.	14.4	Double, (M), flux ratio 1.6:1, p.a. $66^{\circ}$ sep. $40!$ , $D_{\alpha} = 23"$
3 1	604+17W1	16 04 17.39	.12	17 41 19.3	5.9	19.2	2.0	5.4	•
3 1	604+18W1	16 04 01.6		18 23 01		277.	20.	2775	Extended, D= (47",10",20°)
3 1	604+18W2	16 04 31.68	.07	18 08 48.3	3.4	43.6	3.0	8.5	
3 1	604+18W3	16 04 42.29		18 19 27.7		265.	20.	15.5	Extended, D = (21", 7",0°) 4C+18.46
5 1	625+39W1	16 25 01.53	.12	39 46 22.7	8.9	25.6	2.3	8.9	
5 <sub>1</sub>	625+39 <b>W</b> 2	16 25 35.58	.11	39 49 26.9	1.8	18.3	1.1	9.6	
5 i	625+39W3	16 25 36.72	.17	39 47 55.7	3.1	10.8	1.1	6.1	
5 1	625+39W4	16 25 55.47	.20	39 20 28.0	3.6	16.2	1.4	5.4	
4 1	625+40W1	16 25 47.52	.13	40 55 20.3	2.4	13.2	2.2	3.2	
4 1	625+40 <b>W</b> 2	16 25 55.12	.16	40 58 52.9	2.9	9.8	2.2	2.7	
5 1	626+39Wla b	16 26 27.76 16 26 24.82	.11		1.8	49.8 36.1	4. 3.	9.7 7.5	Double (M), D = (37",0",120°)
5 1	626+39W2	16 26 40.59	.16	39 45 12.4	2.9	7.0	0.8	6.3	
	626+39W3 <mark>a</mark> b	16 26 53.7 16 26 55.3		39 39 28 39 39 29		3400.			Extended, D = (31", 8",90°), 3C 338 c.f. Jaffe and Perola (1974)
	626+41W1	16 26 48.25	.15	41 19 37.9	2.7	14.3	3.0	2.8	_
_	627+39W1	16 27 10.91	.04	39 36 11		31.7	1.4	29.0	Extended, D = $(16", 6", 10^{\circ})$
	627+39W2	16 27 14.80	.18	39 25 38.4		9.4	0.8	5.7	
_	627+39W3	16 27 17.28		39 45 29.9		76.2		67.8	
	627+39W4	16 27 24.45		39 50 52.4		19.0		14.2	
	627+39W5	16 27 25.84	.06		1.0	30.2		18.6	
	627+39W6	16 27 32.76		39 37 07.6		54.2		46.0	Extended, D = (23",0",6°)
	627+39W7	16 27 36.87				24.4		18.2	
	627+39W8	16 27 52.04	.05	39 48 22.5	0.9	30.8		21.1	
4 1	627+40W1	16 27 31		40 32 17		85.3	5.	25.1	Extended (M), D = (21",18",0°)

Table 2 (continued)

eld 1)	Name (2)	α (3)	σ <sub>α</sub> (4)	& (5)	σ <sub>δ</sub> (6)	S sky (7)	σ (8)	S	Comments (10)
4	1627+40W2	16 27 47.23	.14	40 54 18.9	3.5	3.3	0.8	3.1	
4	1627+41W1	16 27 18.49	.20	41 12 58.9	3.6	5.7	1.2	2.8	
4	1627+41W2	16 27 44.05	.11	41 05 21.5	2.0	4.8	0.6	3.9	
5	1628+39W1	16 28 24.25		39 28 57		214.	10.	84.0	Extended (M), $D = (23'', 6'', 100^{\circ})$
5	1628+39W2	16 28 49.50		39 29 25		31.3	3.	6.1	Extended,D = (19", 7",50°)
4	1628+40W1	16 28 04.09	.06	40 55 13.7	1.0	7.7	0.6	7.4	
4	1628+40W2	16 28 05.61	.10	40 46 44.2	1.8	5.1	0.6	4.2	
4	1628+40W3	16 28 09.21	.19	40 55 17.5	3.4	2.4	0.6	2.3	
4	1628+40W4	16 28 17.00	.07	40 44 13.4	1.2	8.7	0.6	6.4	
4	1628+40W5	16 28 24.12	.09	40 38 04.5	1.5	9.9	1.0	5.0	
4	1628+40 <b>W</b> 6	16 28 33.92	.06	40 49 29.1	1.0	8.6	0.6	7.3	
4	1628+40 <b>W</b> 7	16 28 46.16		40 56 51.4	1.4	6.7	0.6	5.9	
4	1628+40W8	16 28 50.03	.05	40 52 49.8	0.8	32.2	0.6	26.7	
4	1628+41W1	16 28 28.27	.05	41 12 35.7	0.8	14.3	1.2	8.0	
4	1629+40W1	16 29 38.78	.12	40 57 31.1	2.2	7.0	1.0	3.6	
4	1629+40W2	16 29 57.01	.18	40 22 09.4	3.2	95.2	22.	2.4	
4	1630+40W1	16 30 11.57	.17	40 26 08.4	3.1	76.	17.	2.6	
4	1630+40W2	16 30 31.58		40 59 53.6	2.4	17.5	3.0	3.3	
4	1630+40W3	16 30 32.36	.08	40 52 46.5	1.4	28.5	3.0	5.2	
4	1630+41W1	16 30 16.39		41 03 51.4		9.7	2.4	2.3	
4	1630+41W2	16 30 23.46	.17	41 17 29.4	3.1	30.5	7.	2.6	
4	1630+41W3	16 30 32.87	.13	41 11 47.3	2.3	28.4	6.	3.1	
4	1630+41W4	16 30 36.2		41 02 53		256.	5.	40.7	Extended, $D = (35'', 0'', 37^{\circ})$

# NOTES TO TABLE 2

Column 1: Name of Field containing source; 1 = A1656, 2 = A2147, 3 = A2151, 4 = A2197, 5 = A2199

Column 2: Source name (revised Parkes system)

Column 3: Right Ascension (1950)

Column 4: rms error in R.A.

Column 5: Declination (1950)

Column 6: rms error in Dec.

Column 7: Source Sky Flux density in mJy

Column 8: rms error in Sky Flux

Column 9: Source Map Flux

Column 10: Comments, including source name in other catalogues, description of extension parameters, (M) = contour map of source reproduced in figure 5.

Table 3

Name (1)	position error (2)	α <sub>0</sub> (3)	δ <sub>0</sub> (4)	$\begin{array}{cccc} \alpha_0 & \alpha_r & \delta_0 & \delta_r \\ (5) & (6) \end{array}$	Class (7)	Comments (8)
1254+27W1	1.8x3.2	12 54 58.99	27 46 6.6	-0.9 -2.3	I	N4839, E galaxy, $m_p^a = 13.6$ , $v^b = 7376$ (F)
1254+28Wla,	b	12 54 12.1	28 32 5.2		II	Blue object, m <sub>B</sub> =20 (M)
1255+27W1	2.8x5.7	12 55 29.58	27 53 12.0	-2.3 -5.9	I	E galaxy, $m_{v} = 16$ , $v^{b} = 20256$ (F)
1255+27W2a,	Ъ	12 55 47.01	27 50 59.4		II	m <sub>V</sub> =20 object (M)
1255+28W1	1.2x1.7	12 55 20.25	28 13 53.4	-0.1 -3.8	I	m <sub>G</sub> = 21 object (F)
1255+28W3	3.5x7.2	12 55 32.78	28 19 52.7	+10.2 +3.7	II	Galaxy, E(?), irregular envelope, $m_{\tilde{V}}=15$ , $v^{D}=8151$ (F)
1255+28W4Ъ	1.3x1.7	12 55 37.08	28 36 12.5	0.0 -1.3	I	Blue object, m <sub>R</sub> = 19 (F)
1255+28W5	3.1x6.3	12 55 40.07	28 6 34.5	+10.6 +6.9	III	m <sub>C</sub> = 21 object (F)
1255+28W6	1.4x2.2	12 55 40.69	28 30 44.4	+0.8 -4.7	I	N4848, Ir galaxy, $m_p^a = 14.2$ , $v^b = 7271$ (F)
1255+28W7	1.4x2.2	12 55 47.14	28 43 57.4	0.0 -2.6	I	m <sub>C</sub> = 21 object (F)
1256+27W4	3.2x6.6	12 56 40.33	27 54 56.4	+1.3 +6.2	I	RB 219 <sup>h</sup> , SB galaxy, m <sub>p</sub> <sup>a</sup> =15.1, v <sup>b</sup> =5354 (F)
1256+28W2	3.0x6.1	12 56 28.03	28 10 48.1	-2.5 -5.0	I	Galaxy, peculiar, m <sub>V</sub> =18 (F)
1256+28W4a,	Ъ	12 56 32.78	28 3 19.8		III	RB 214 <sup>h</sup> , SO galaxy, m <sub>V</sub> =16, v <sup>b</sup> =6975 (M)
1256+28W7		12 56 37.28	28 23 6.0	+0.5 +0.8	II	N4858, SB galaxy, $m_p^a = 15.5$ , $v^b = 9491$ (F)
1256+28W8	2.4x4.6	12 56 55.19	28 21 13.9	-0.5 -1.5	I	N4865, E galaxy, m <sub>p</sub> =14.6, v <sup>b</sup> =4588 (F)
1256+28W9		12 56 56.83	28 10 53.3		II	N4869 c.f. Jaffe and Perola (1974)
1257+27W2	1.3x2.0	12 57 42.02	27 45 46.8	- 0.9 + 2.2	I	Galaxy, m <sub>V</sub> =19 (F)
1257+28W1		12 57 11.25	28 13 47.6	-	I	N4874 c.f. Jaffe and Perola (1974)
1257+28W2	3.2x6.6	12 57 40.82	28 4 37.1	+ 7.9 +18.2	III	Lenticular galaxy, m <sup>a</sup> <sub>p</sub> =15.7, v <sup>b</sup> =6636 (F)
1258+28W2	1.7x2.9	12 58 4.15	28 46 17.1	+ 2.9 - 2.3	I	QSO, m <sub>B</sub> =18, z <sup>c</sup> =0.645 (F)
1258+28W3	1.5x2.3	12 58 13.56		+ 2.2 + 2.2	Ι	IC4040, I/Sc galaxy, m <sup>a</sup> =15.1, v <sup>b</sup> =7644 (F)
1258+28W6	2.2x4.4	12 58 30	28 3 30 <sup>T</sup>			N4911, Sc galaxy, m <sub>p</sub> <sup>a</sup> =13.7, v <sup>b</sup> =7898 (F)
1559+15W2	2.8x8.8	15 59 56.23		+ 4.9 -13.7	I	m <sub>G</sub> = 21 object (M)
1559+16W1	2.8x8.8	15 59 56.95		+ 1.0 + 8.7	I	Galaxy in triple system, m <sub>V</sub> =15.5 (M)
1600+15W2		16 00 20.27			III	Object closest to radio peak, m <sub>V</sub> =18.5 (M)
1559+16W2a,	<b>,</b> b	15 59 59.96			II	Arp 324, E galaxy, $m_p^{a=14.9}$ , $v^{d=10483}$ (M)
1600 +16W1	1.1x2.0	16 00 01.85	16 15 28.6	+ 5.5 + 1.1	III	Blue object close to radio peak, m <sub>B</sub> =19 (F)
1600+16W6	2.6x8.4	16 00 38.51	16 37 21.3	+ 1.3 +25.2	III	$m_{V}^{-19.5}$ object (F)
1600+16W7	2.9x9.3	16 00 40.87	16 28 43.2	- 4,6 -20.5	I	Galaxy m <sub>V</sub> =17 (Fa)
1600+16W8	2 69 /	16 00 41.21 16 00 41.70		+ 0.3 +27.2	I I	m <sub>v</sub> =18.5 object (Fb)
1000110#0	2.6x8.4	16 00 41.70		- 1.1 - 2.4 - 3.7 +19.7	I	m <sub>V</sub> = 20 object (Fa) m <sub>C</sub> =21 object (Fb)
1600+16W10	1.6x4.3	16 00 58.16		+ 2.9 + 0.5	I	Galaxy, E compact, m <sub>n</sub> <sup>a</sup> =15.5 (F)
1600+16W11		16 00 58.05	16 12 02.3		II	m <sub>vr</sub> =16 star (Ma)
		16 00 58.94			II	m <sub>v</sub> =17 star (Mb)
1601+15Wla	<b>,</b> b	16 01 26	15 55 52		III	Double Galaxy, m <sub>V</sub> =16,17 (M)
1601+15W2	1.2x2.2	16 01 41.00	15 55 47.2	- 1.0 + 3.1	I	Bluish object, m <sub>B</sub> =19.5 (F)
16Q1+16W3	1.1x2.0	16 01 20.94	16 02 17.3	+ 0.4 + 1.2	I	Galaxy, E (?) with companion, m <sub>v</sub> =15.5 (F)
1602+16W4	1.9x5.5	16 01 25.93	16 12 35.7	- 4.0 - 1.1	I	$m_{V}$ =20 object in proximity of $16^{m}$ lenticular galaxy
1601+16W5	1.1x2.0	16 01 35.78	16 28 04.5	- 1.6 - 7.6	III	m <sub>w</sub> =20 object (F)
1601x16W6	1.4x3.4	16 01 51.17		+ 2.6 - 4.9	I	Peculiar galaxy, m <sub>tt</sub> =17.5 (F)
1601+17W1	1.4x3.4	16 01 16.18		- 1.1 - 0.1	I	N6034, E galaxy, m <sub>n</sub> =15.2 (F)

<sup>†</sup> Position not measured. Position given from Zwickey and Herzog (1963).

Table 3 (continued)

Name (1)	position error (2)	α <sub>ο</sub> (3)	δ <sub>ο</sub> (4)	α <sub>o</sub> -α <sub>r</sub> (5)	δ <sub>0</sub> -δ <sub>r</sub> (6)	Class (7)	Comments (8)
1602+15W1	1.1x2.0	16 02 13.56	15 54 31.3	+ 0.6	+ 1.3	I	$m_{\overline{V}}^{=18.5}$ object (F)
1602+16W2	2.0x6.0	16 02 10.45	16 08 55.9	+ 8.1	+ 3.2	III	Galaxy, m <sub>V</sub> =17.5 (F)
1602+16W4	2.0x6.0	16 02 39.39	16 18 46.0	- 0.1	- 3.5	I	m <sub>V</sub> =20 object (F)
1602+17W1	1.1x2.0	16 02 11.40	17 52 39.1	- 0.1	- 0.3	I	N6040B, galaxy SABO/a pec <sup>f</sup> , $m_p^a$ : 15 with an SAB(s)cd pec <sup>f</sup> companion, $v^g$ =12508 (F)
1602+17W2	1.6x4.8	16 02 20.74 16 02 19.84	17 51 25.1 17 51 10.4	+ 3.3 - 9.6	+11.7	II	N6041A,B, two galaxies in one envelope, SABO and SBO <sup>-f</sup> , $m_p^a$ =15, $v^e$ =10561 (F)
1602+ 17W3	1.2x2.6	16 02 21.32	17 41 32.6	- 0.3	+ 4.2	I	Bluish object, m <sub>B</sub> =19.5 (F)
1602+17W4		16 02 54.00	17 51 53.2			I	N6047 c.f. Jaffe and Perola (1974)
1602+18W1		16 02 10.38	18 11 24.5	- 6.9	- 0.3	II	$m_{V} = 16 \text{ star (Fa)}$
		16 02 11.02	18 11 23.0	+ 2.3	- 1.8	II	m <sub>G</sub> = 21 object (Fb)
1603+17W2	2.8x8.8	16 03 21.86	17 56 11.4	- 2.0	-14.3	I	IC1182, SO or E galaxy with blue jet, m <sub>p</sub> <sup>a</sup> =15.2 (F)
1603x17W3	1.6x4.5	16 03 29.67	17 51 04.1	- 3.4	+21.2	III	IC1185, E galaxy, $m_p^a = 15.1$ , $v^e = 10575$ (F)
1603+18WI	1.8x5.0	16 03 11.41	18 03 33.2	- 2.7	-14.4	III	$m_{V}^{-18}$ star (F)
1603+18W2		16 03 26.05	18 20 25.7			III	$m_{V}^{=19}$ object (M)
1604+18W1	1.2x2.6	16 04 01.57	18 23 00.1	- 0.4	- 1.5	I	N6061, SO or E galaxy, with two compact companions, $m^a_p=15.0$ , $v^e_p=11292$ (F)
1625+39W2	1.6x2.2	16 25 34.38	39 49 26.4	- 1.6	- 0.2	I	Red galaxy with plume, $m_{\overline{V}}$ =18.5 (F)
1626+39Wla,b		16 26 26.77	39 13 34.8			II	$m_{V}^{=19.5}$ object 10" from radio axis (M)
1626+39W2	2.1x3.1	16 26 40.65	39 45 12.7	+ 0.6	+ 0.3	I	$m_{\overline{V}}$ =17.5 object (F)
1626+39W3ab		16 26 55.35	39 39 36.4			I	N6166 c.f. Jaffe and Perola (1974)
1626+41W1	2.0x2.9	16 26 48.33	41 19 41.4	+ 0.9	+ 3.5	I	Complex galaxy, $m_p^a = 14.3$ (F)
1627+39W1	1.1x1.3	16 27 11.07	39 36 11.2	+ 1.7	- 0.2	I	Galaxy, $m_{\overline{V}} = 20$ (F)
1627+39W2	2.3x3.3	16 27 14.75	39 25 39.4	- 0.6	+ 1.0	I	RS 108 <sup>1</sup> SO galaxy, m <sub>V</sub> =15 (F)
1627+39W7	1.3x1.7	16 27 37.02	39 32 13.1	+ 1.7	-12.5	III	RS 116 <sup>i</sup> SBO galaxy, $m_V^{=15}$ , $v^{\hat{j}}$ =8378 (F)
1627+40W1		16 27 31.15 16 27 32.03	40 32 20.4 40 32 23.9			II	m <sub>V</sub> =20 objects (Ma,b)
1627+41W1	2.5x3.7	16 27 18.74	41 13 00.7	+ 2.8	+ 1.7	I	m <sub>v</sub> =20 object (F)
1628+39W2		16 28 49.76	39 29 26.7			II	RS 147 <sup>i</sup> SO galaxy, m <sub>V</sub> *15.5 (F)
1628+40W1	1.2x1.4	16 28 04.31	40 55 10.4	+ 2.5	- 3.3	11	N6173, E galaxy, m <sup>a</sup> =14.0 (F)
1628+40W4	1.3x1.6	16 28 16.91	40 44 15.5		+ 2.1	I	N6175, lenticular + E galaxy, m <sup>a</sup> <sub>p</sub> =15.0; radio source coincides with centre of lenticular (F)
1628+40W6	1.2x1.4	16 28 33.98	40 49 26.5	+ 0.6	- 2.6	I	m <sub>U</sub> =17.5 object (F)
1629+40W1	1.7x2.4	16 29 39.02	40 57 30.1	+ 2.7	- 1.0	I	Galaxy, m <sub>V</sub> =19.5 (F)
1629+40W2	2.3x3.3	16 29 57.25	40 22 04.0	+ 2.7		ı	m <sub>v</sub> =20 object (F)
					- 5.4		<b>Y</b>
1630+41W2	2.2x3.2	16 30 23.94	41 17 23.4	+ 5.4	- 6.0	III	m <sub>V</sub> =20 object (F)

Table 4

Coma. Number	of object	s per uni	t area = 4	x 10 <sup>-4</sup>	arcsec <sup>-2</sup>	
	NURS	NEI	NI			
$0^{8}.25 - 0^{8}.20$	6	1.4	4			
0 .20 - 0 .15	8	1.2	1			
0 .15 - 0 .10	9	0.7	2			
0 .10 - 0 .04	10	0.4	6			
total	33	3.7	13			
A2147+2151. Nu	mber of o	bjects pe	r unit are	a = 6.5	ж 10 <sup>-4</sup> а	rcsec_
0 <sup>8</sup> .19 - 0 <sup>8</sup> .15	8	3.3	8			
$0^8.19 - 0^8.15$ $0.15 - 0.10$	-	3.3 2.2	8 2			
	9		-			
0 .15 - 0 .10	9 24	2.2	2			
0 .15 - 0 .10 0 .10 - 0 .03	9 24 41	2.2 2.4 7.9	2 8 18	rea ≖ 4	ж 10 <sup>-4</sup> г	urcsec
0 .15 - 0 .10 0 .10 - 0 .03 total	9 24 41	2.2 2.4 7.9	2 8 18	rea ≖ 4	ж 10 <sup>-4</sup> г	_ urcsec
0 .15 - 0 .10 0 .10 - 0 .03 total	9 24 41 *********************************	2.2 2.4 7.9 objects	2 8 18 per unit a	rea = 4	ж 10 <sup>-4</sup> г	rcsec -
0 .15 - 0 .10 0 .10 - 0 .03 total A2197 + 2199. 1	9 24 41 **Wumber of	2.2 2.4 7.9 Objects 1	2 8 18 per unit a	rea = 4	х 10 <sup>-4</sup> г	rcsec

NURS = number of radio sources

NEI - number of expected chance identifications

NI = number of identifications found

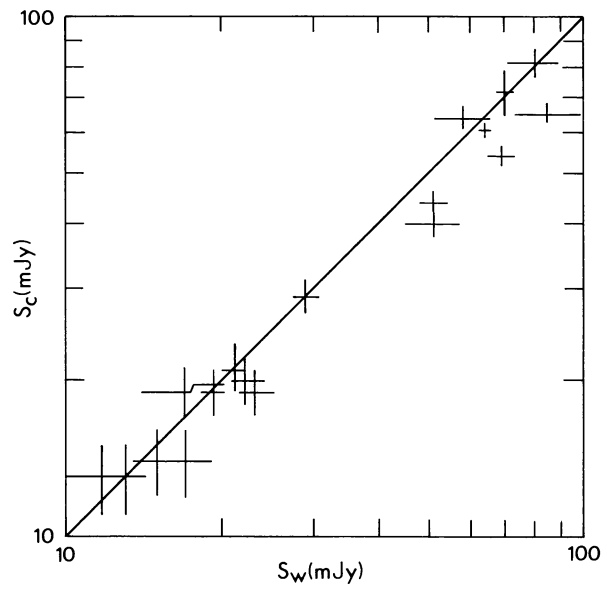


Figure 1 1407 MHz fluxes measured with the Cambridge Half-Mile Telescope (Gillespie 1974) plotted against 1415 MHz fluxes measured with the WSRT for sources in common in the 504 survey and this survey. The bars show the reported mean errors in the flux measurements.

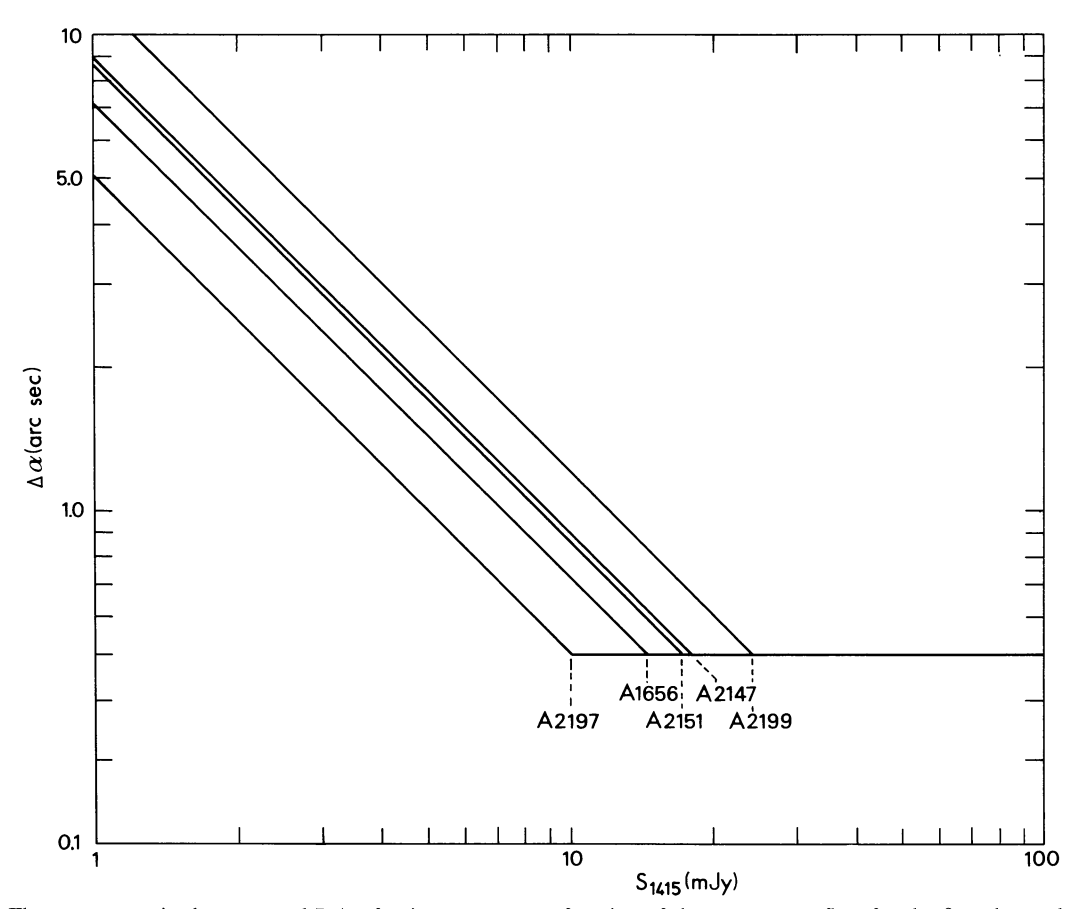


Figure 2 The mean error in the measured R.A. of point sources as a function of the source map flux, for the five observed fields. The mean error in Dec. is greater by a factor csc  $\delta$ .

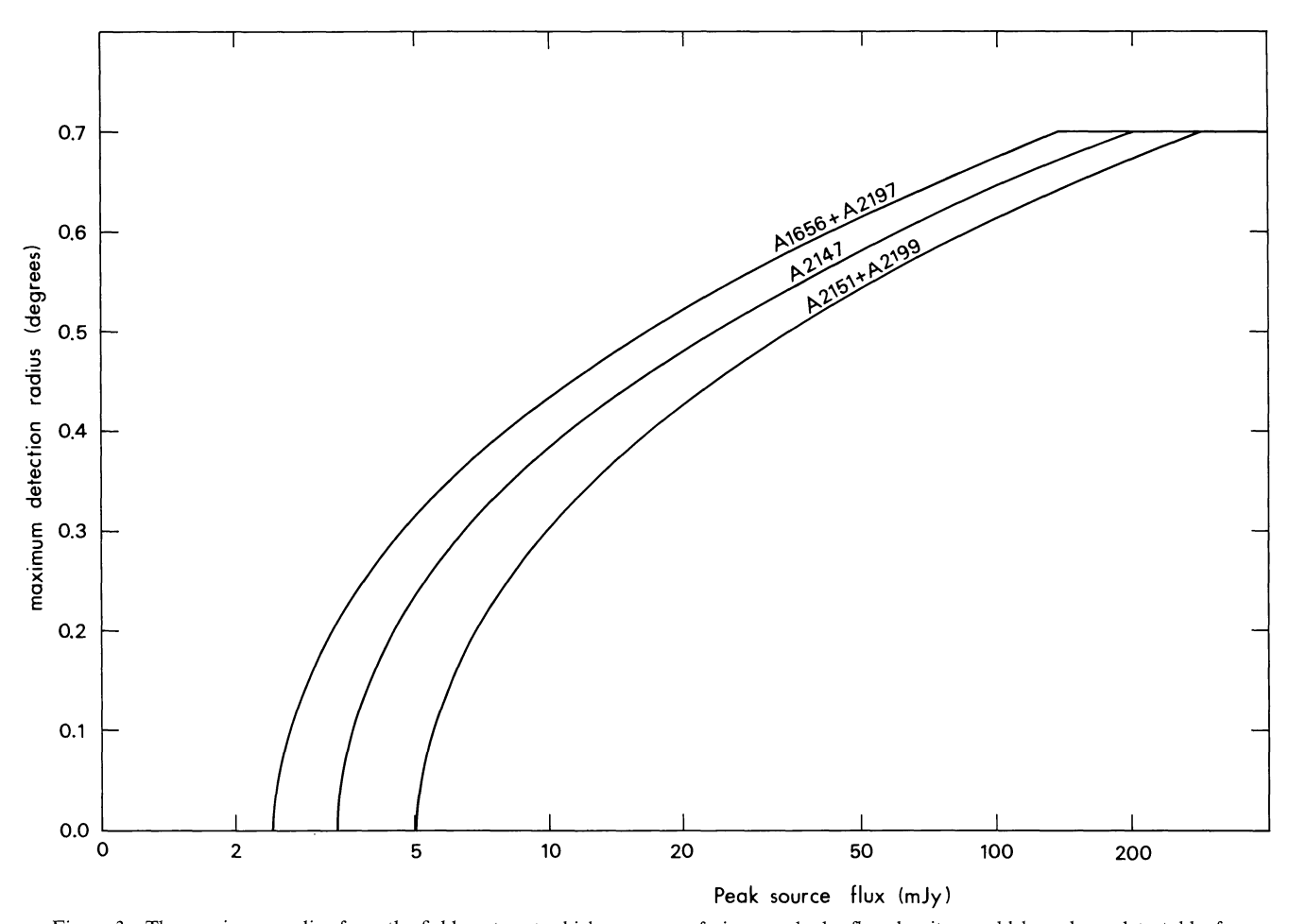


Figure 3 The maximum radius from the field center at which a source of given peak sky flux density would have been detectable, for each observed field. The peak flux density of an extended object is the maximum flux density measured over a solid angle corresponding to the size of the synthesized beam.

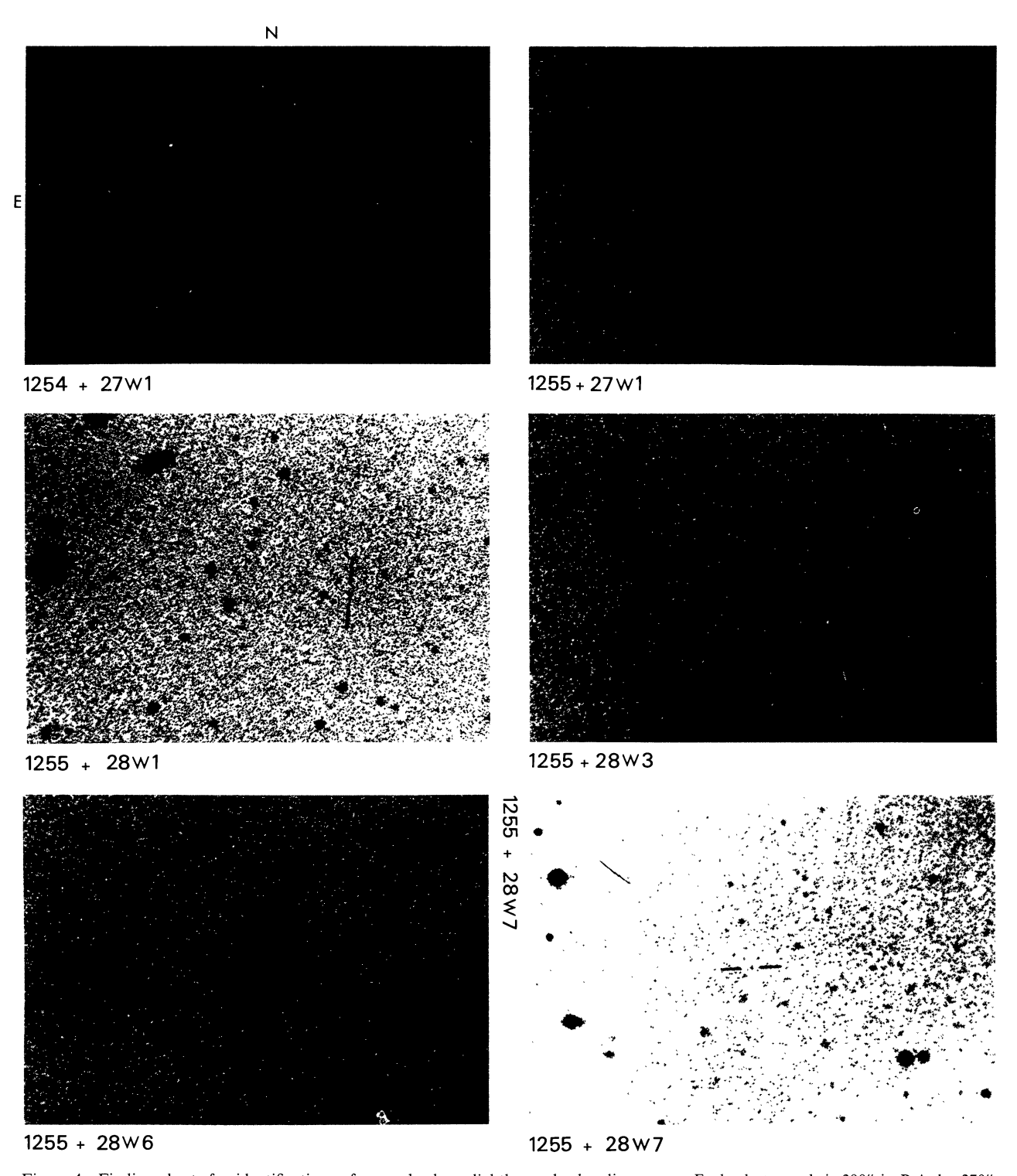


Figure 4 Finding charts for identifications of unresolved or slightly resolved radio sources. Each photograph is 390" in R.A. by 270" in Dec. and is printed with north upwards and east on the left, with the exception of 1255+28W7 which has been rotated 90° clockwise. The double bars indicate objects listed in table 3. For galaxies of large angular size, four bars are drawn which give the probable position of the radio source within the galaxy.

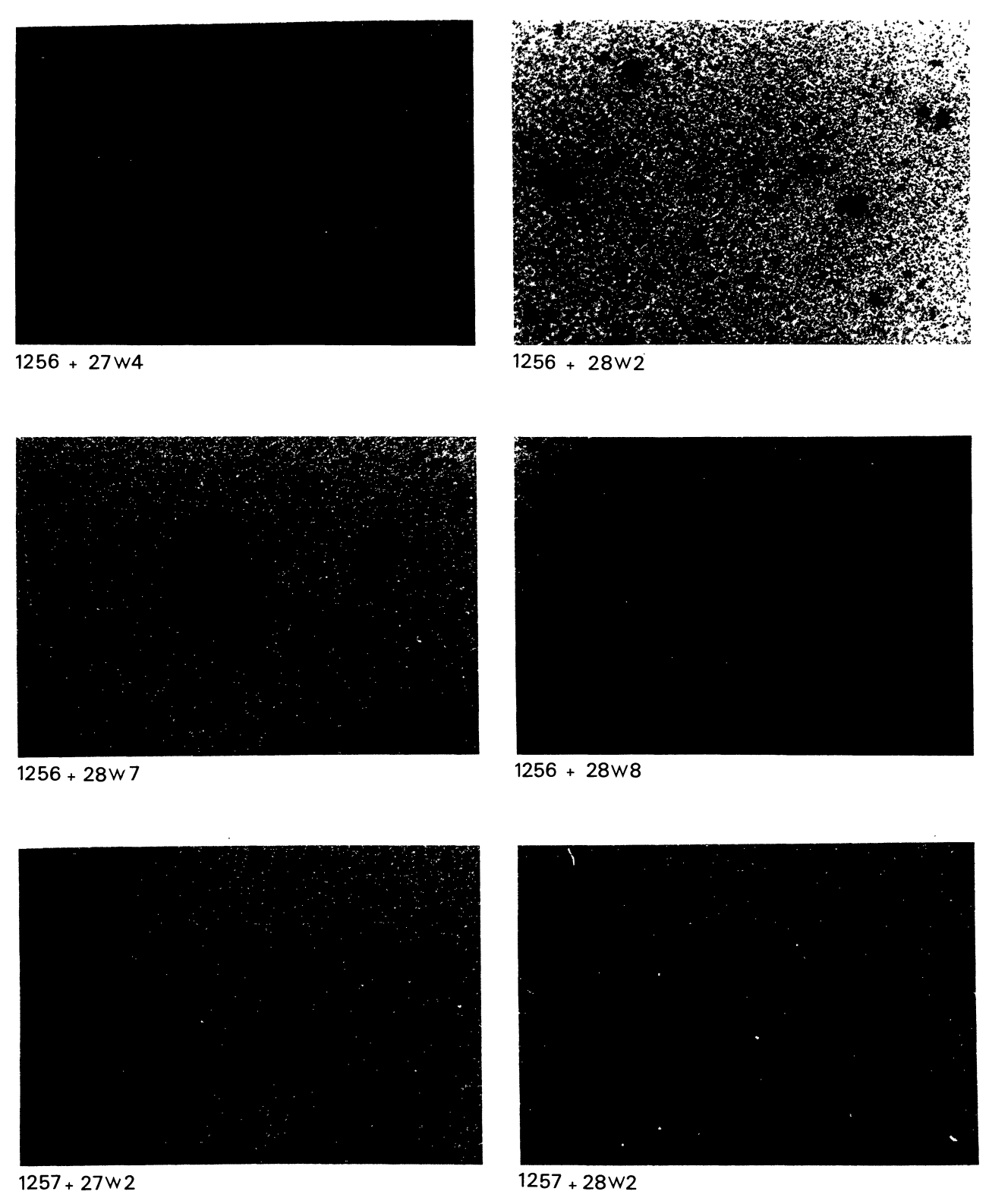


Figure 4 (continued)

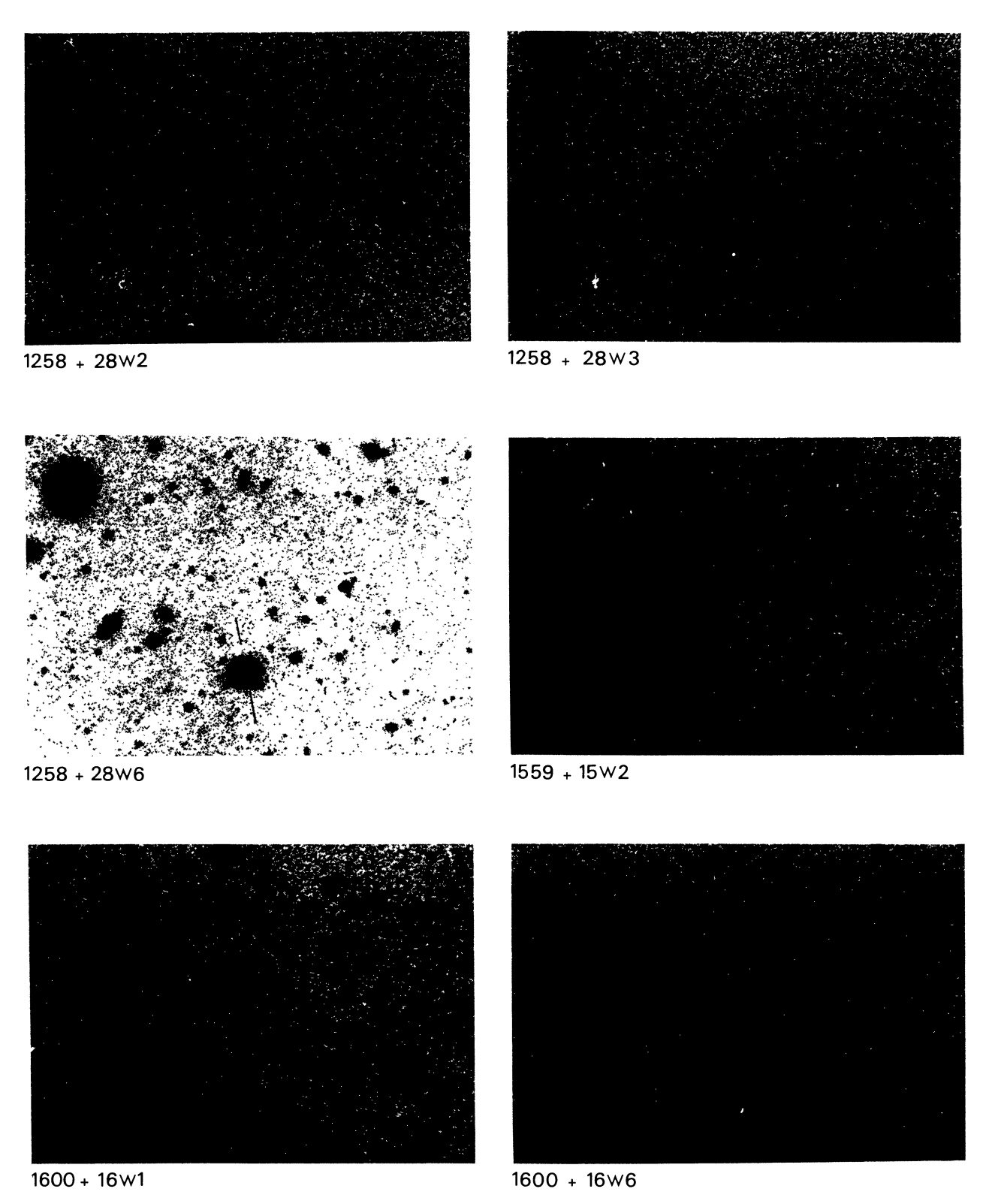


Figure 4 (continued)

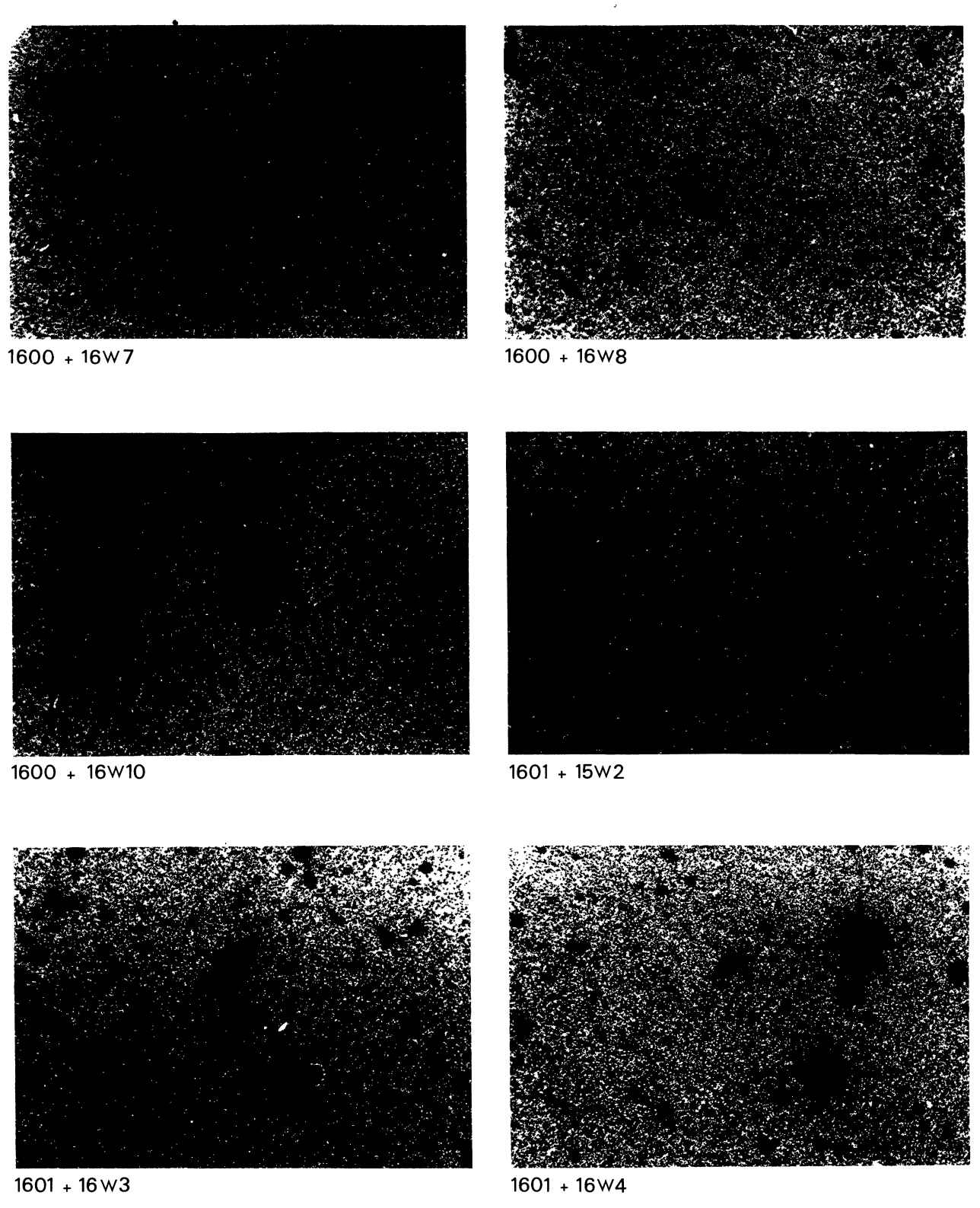


Figure 4 (continued)

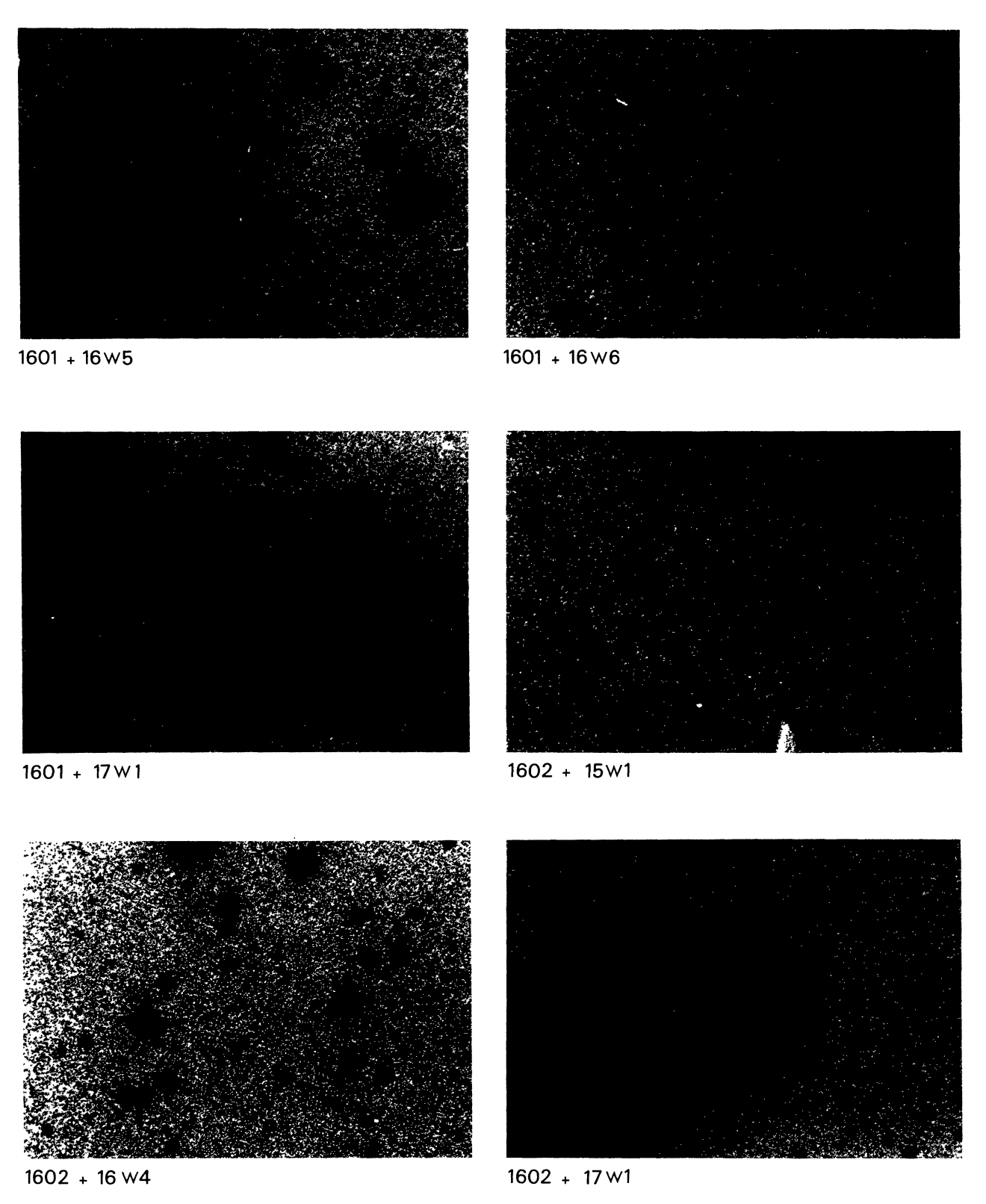


Figure 4 (continued)

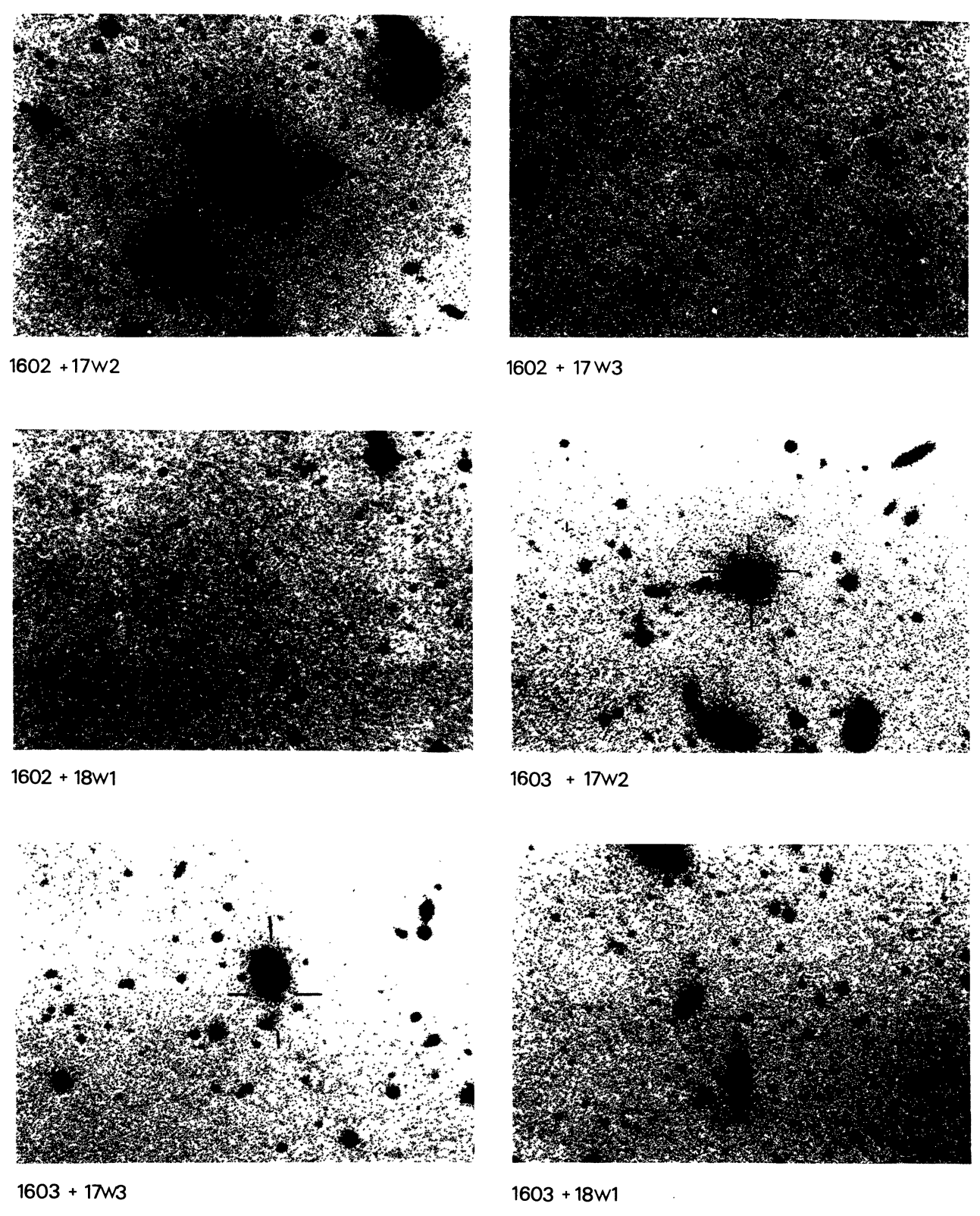


Figure 4 (continued)

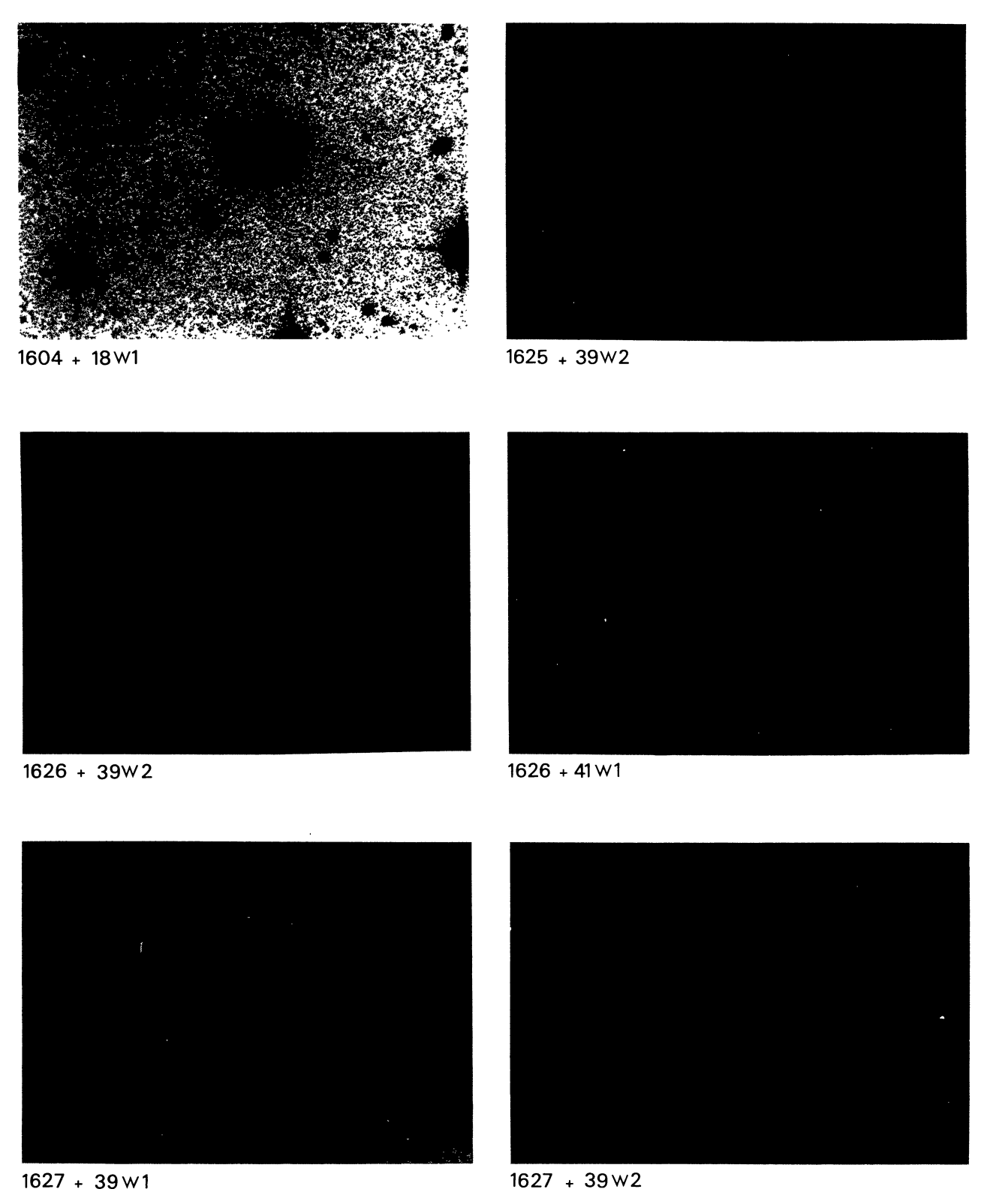


Figure 4 (continued)

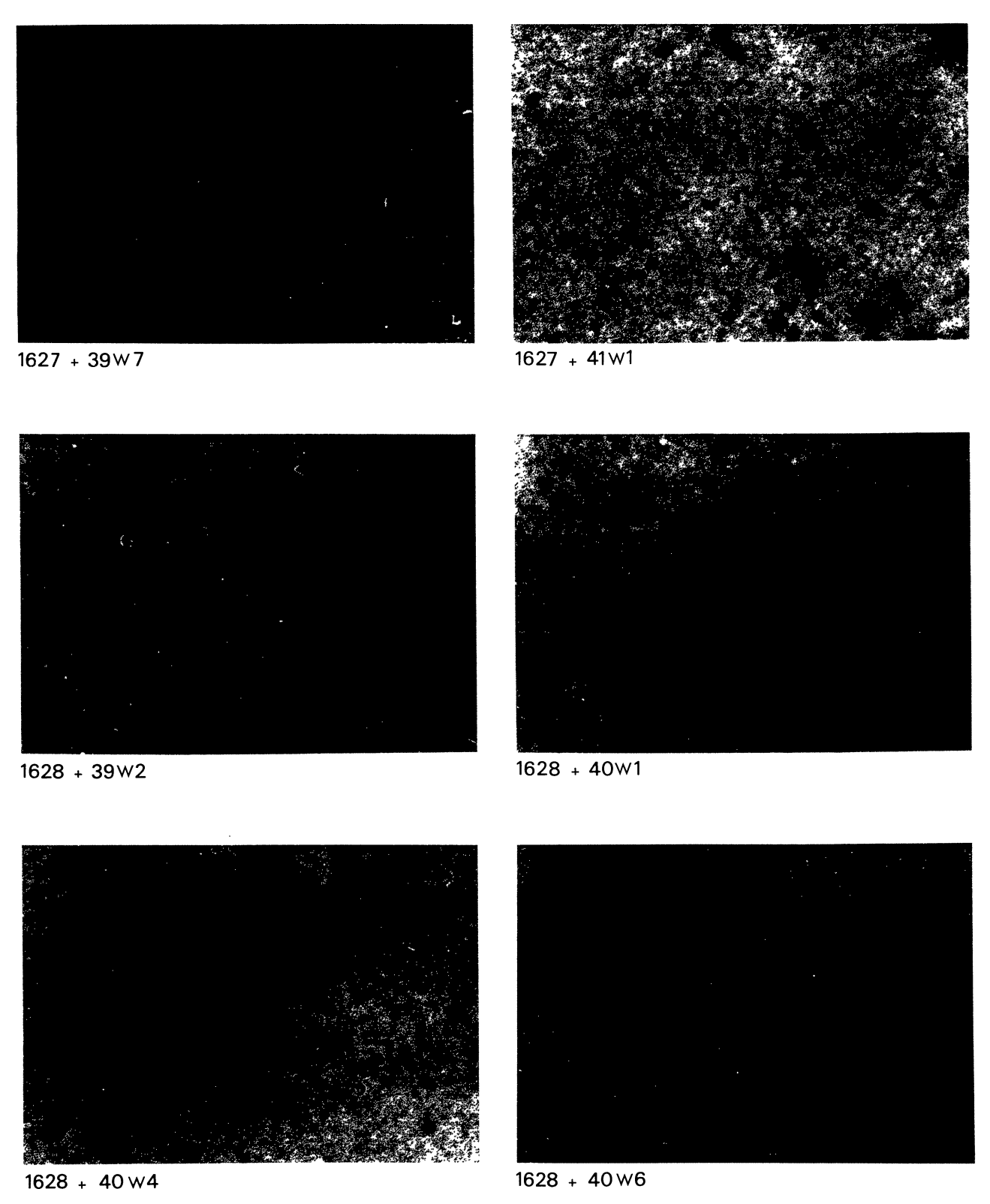
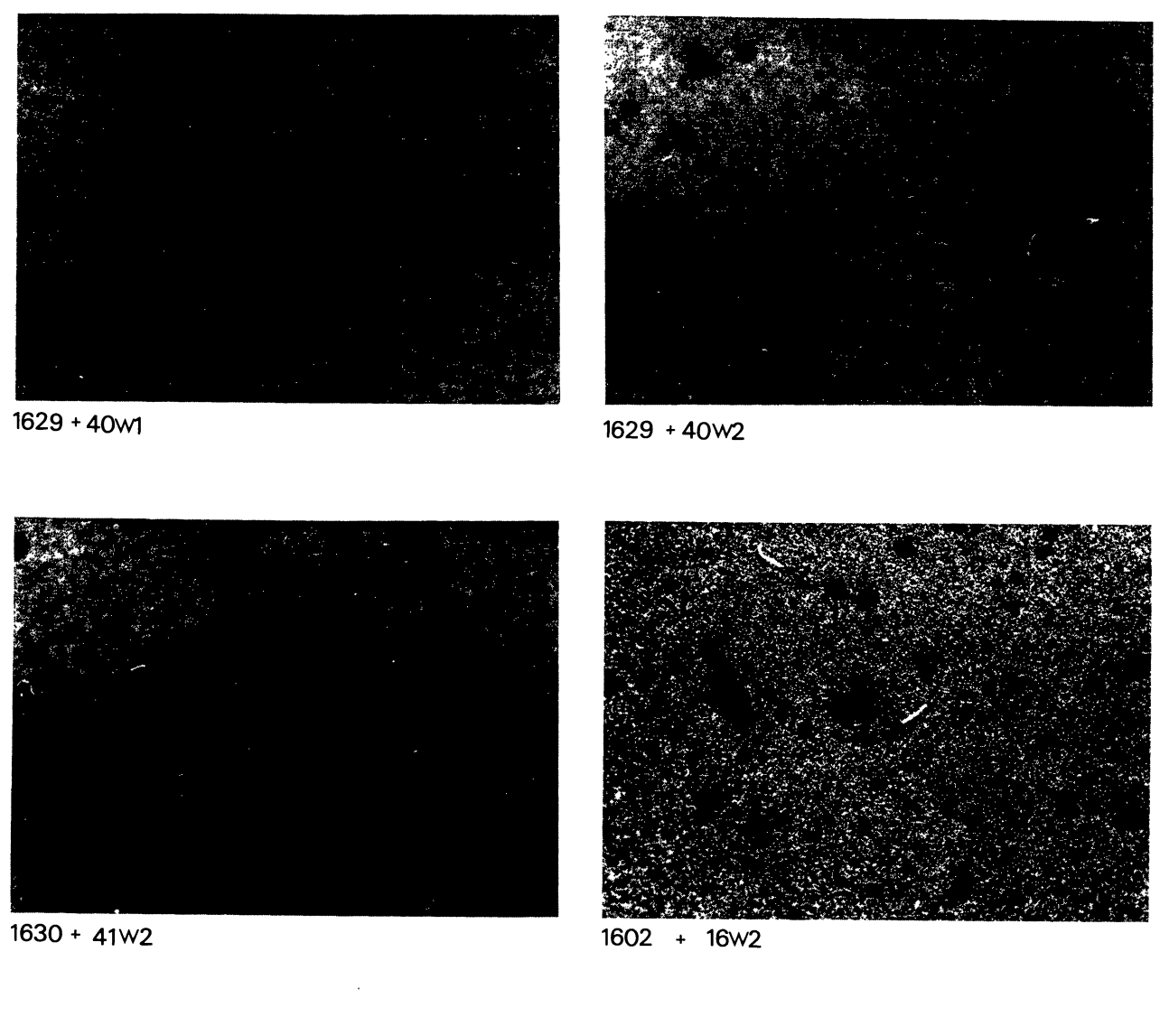


Figure 4 (continued)



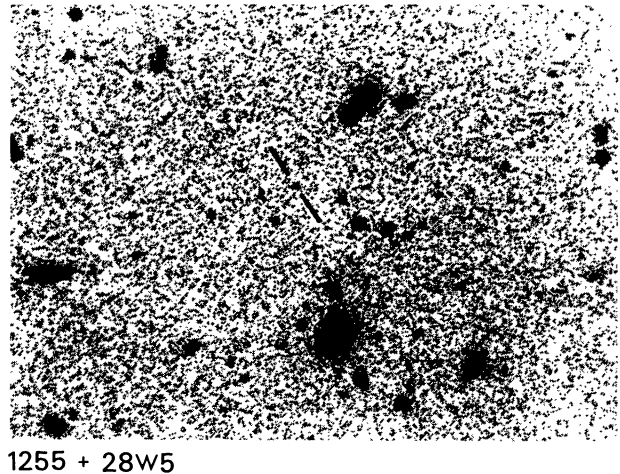
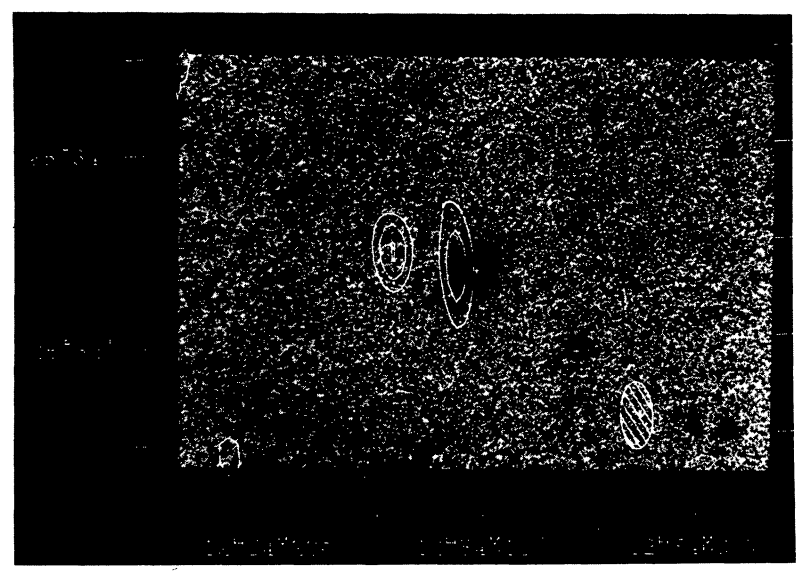
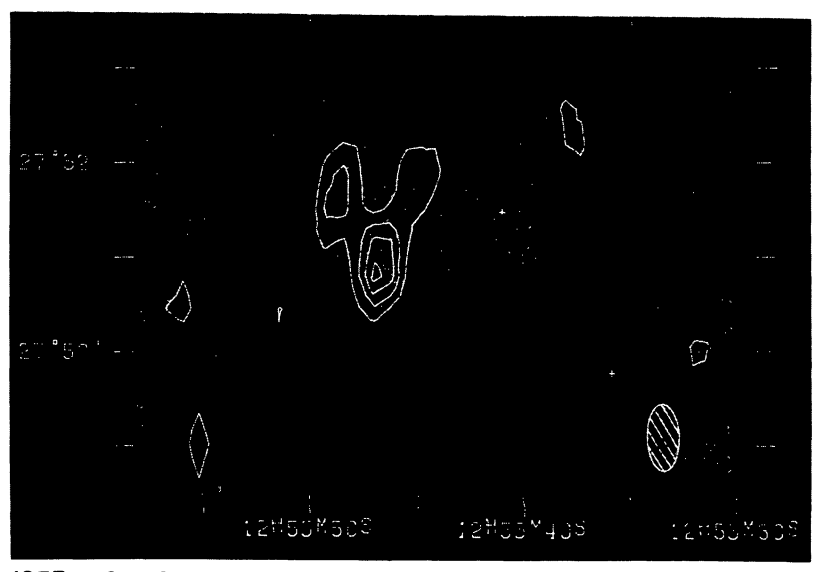


Figure 4 (continued)



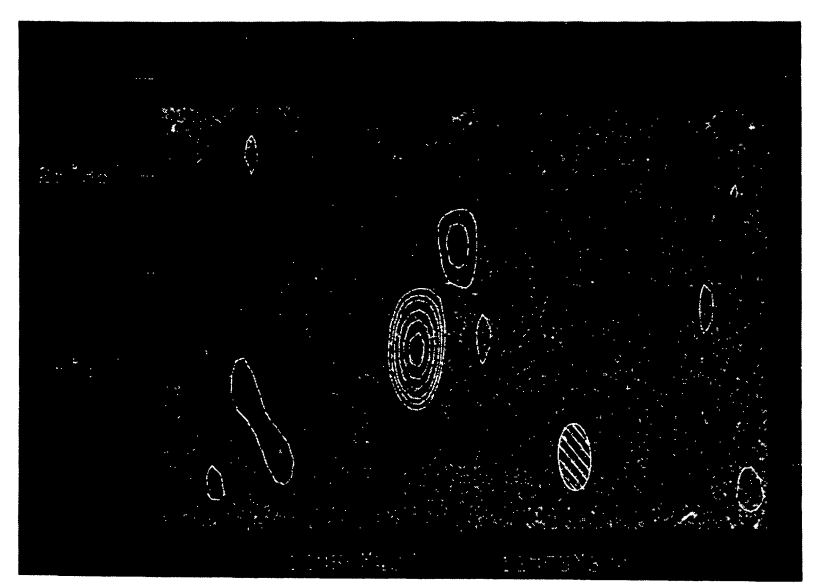
1254 + 28W1



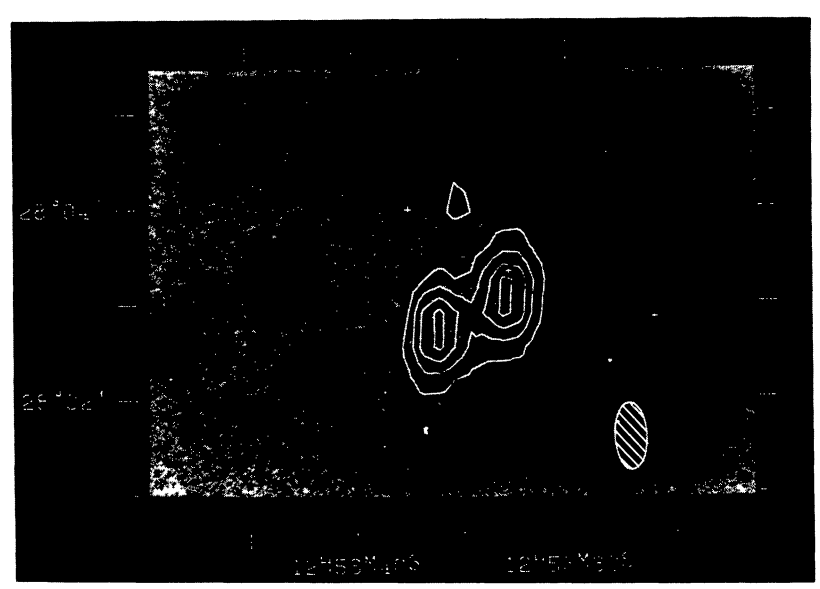
1255 + 27W2

Figure 5 Contour maps and finding charts of extended radio sources. FWHM synthesized beamwidths are given by the hatched ellipses. The small white crosses indicate secondary reference stars used to determine positions on the photographs. Contour values (c.v.) given below are in mJy per synthesized beam. The beam areas (b.a.) given below are the main beam solid angles in units of  $10^{-8}$  steradians.

- a) 1254 + 28W1, c.v. = (30,50,70,90), b.a. = 2.3, bars give identification from table 3.
- b) 1255 + 27W2, c.v. = (4,9,14,19), b.a. = 2.3



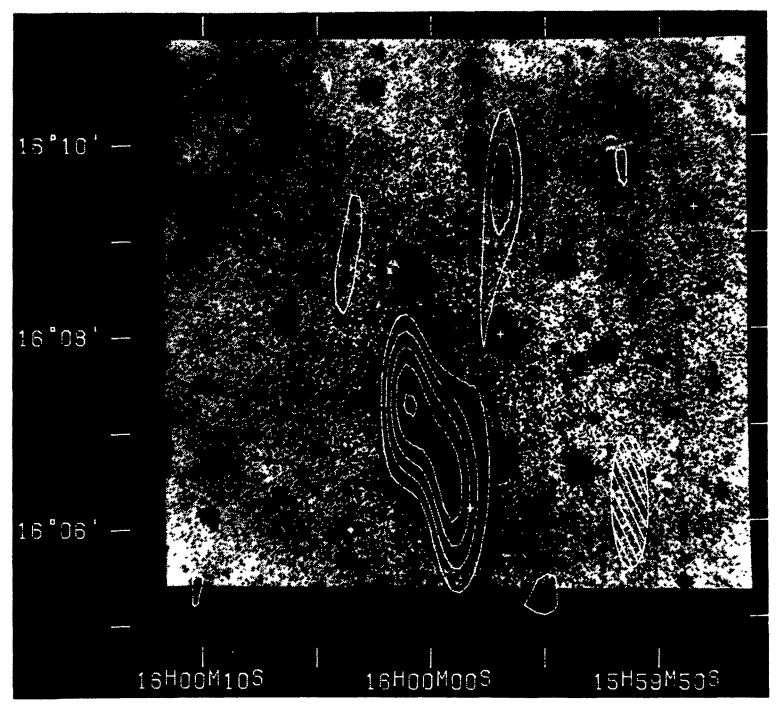
1255 + 28 W4



1256 + 28W4

Figure 5 (continued)

- c) 1255 + 28W4, c.v. = (6,11,16,26,36,46), b.a. = 2.3
- d) 1256 + 28W4, c.v. = (3.9, 15.21), b.a. = 2.3



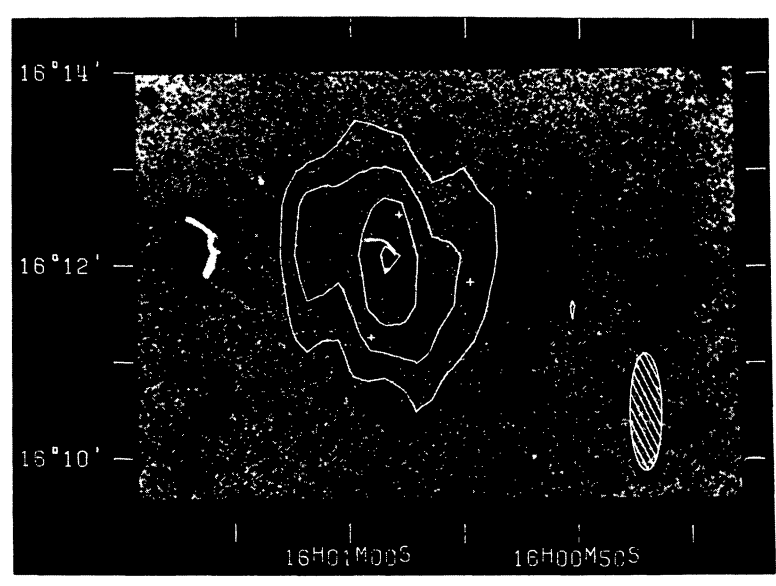
1559 + 16W1 - 1559 + 16W2



1600 + 15 W 2

Figure 5 (continued)

- e) 1559 + 16W1/W2, c.v. = (3,5,5.5,7.5,9.5,11.5), b.a. = 3.0
- f) 1600 + 15W2, c.v. = (10,20,30,60,90,120), b.a. = 3.0



1600 + 16W11

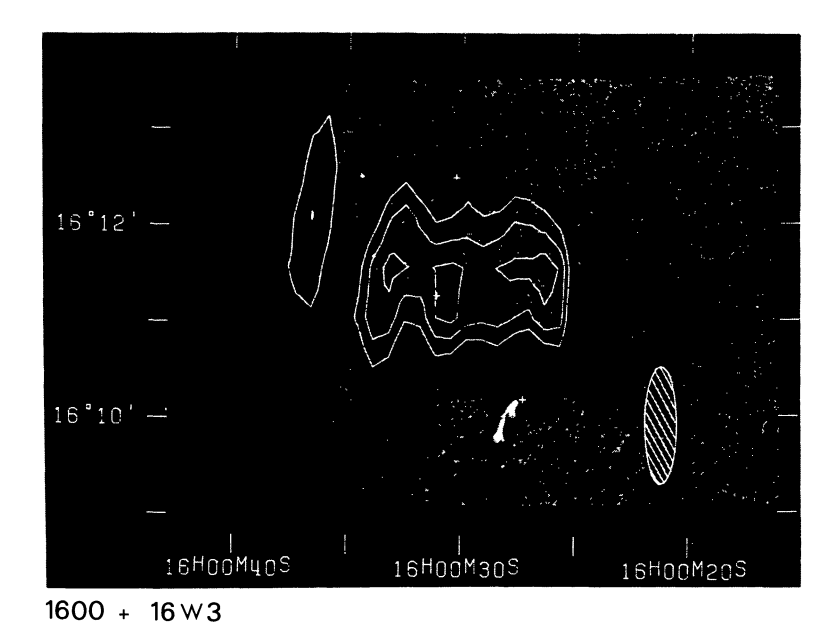
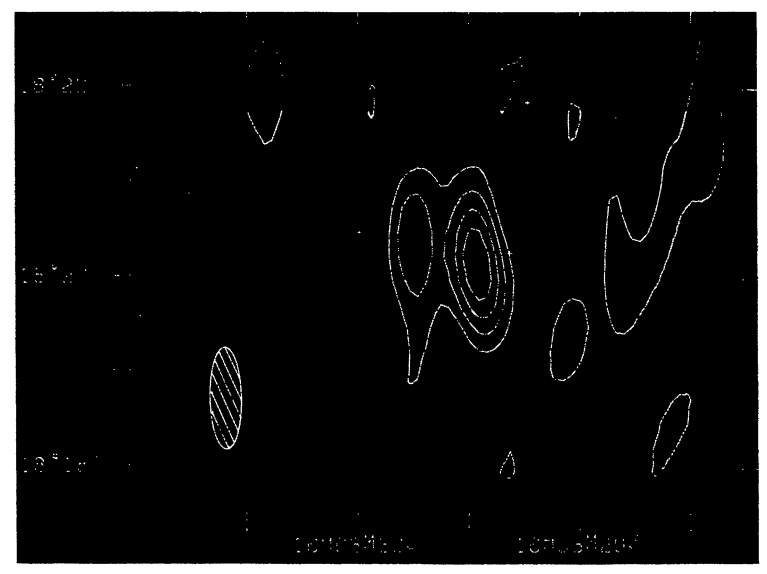
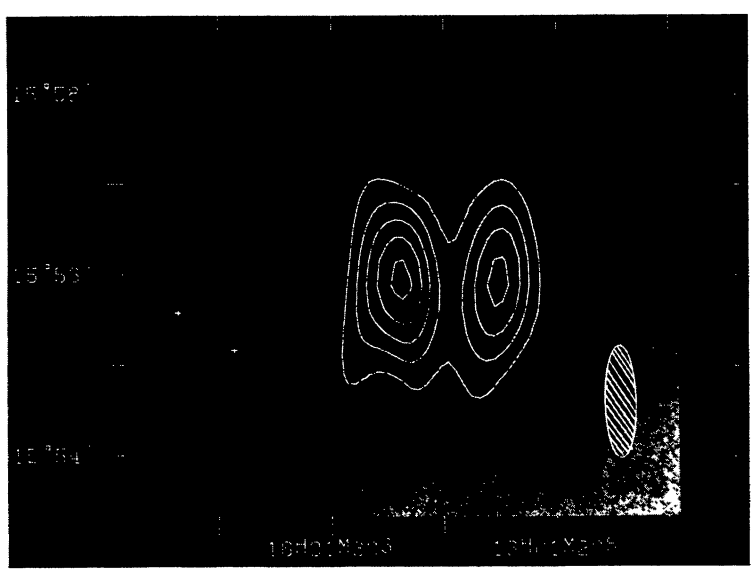


Figure 5 (continued)

- g) 1600 + 16W11, c.v. = (2,4,6,8), b.a. = 3.0
- h) 1600 + 16W3, c.v. = (2,3,4), b.a. = 3.0



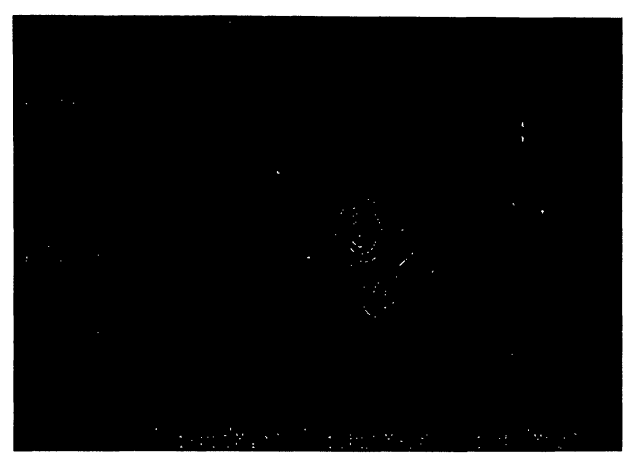
1603 + 18W2



1601 + 15W1

Figure 5 (continued)

- i) 1603 + 18W2, c.v. = (5,12,19,26), b.a. = 3.0
- j) 1601 + 15W1, c.v. = (5,12,19,26,33), b.a. = 3.0





1627 + 40W1 1626 + 39W1



Figure 5 (continued)

- k) 1627 + 40W1, c.v. = (5,15,25,35,45), b.a. = 1.7
- 1) 1626 + 39W1, c.v. = (3,10,17,24,31,38), b.a. = 1.7
- m) 1628 + 39W1, c.v. = (20,40,60,80), b.a. = 1.7